ACS OMEGA

http://pubs.acs.org/journal/acsodf

Article

Can 2-Pyridyl-1,2,3-triazole "Click" Ligands be Used to Develop Cu(I)/Cu(II) Molecular Switches?

Daniel A. W. Ross, James A. Findlay, Roan A. S. Vasdev, and James D. Crowley*

Cite This: *ACS Omega* 2021, 6, 30115−30129

Read Online

ACCESS | Metrics & More | Article Recommendations | Supporting Information

ABSTRACT: Molecular switching processes are important in a range of areas including the development of molecular machines. While there are numerous organic switching systems available, there are far less examples that exploit inorganic materials. The most common inorganic switching system remains the copper(I)/copper(II) switch developed by Sauvage and co-workers over 20 years ago. Herein, we examine if bidentate 2-(1-benzyl-1*H*-1,2,3-triazol-4-yl)pyridine (pytri) and tridentate 2,6-bis[(4-phenyl-1*H*-1,2,3-triazol-1-yl)methyl]pyridine (tripy) moieties can be used to replace the more commonly exploited polypyridyl ligands 2,2′-bypyridine (bpy)/1,10-phenanthroline (phen) and 2,2′;6′,2″-terpyridine (terpy) in a copper(I)/(II) switching system. Two new ditopic ligands that feature bidentate (pytri, **L1** or bpytri, **L2**) and tridentate tripy metal binding pockets were synthesized and used to generate a family of heteroleptic copper(I) and copper(II) 6,6′-dimesityl-2,2′-bipyridine (diMesbpy) complexes. Additionally, we synthesized a series of model copper(I) and copper(II) diMesbpy complexes. A combination of techniques including nuclear magnetic resonance (NMR) and UV−vis spectroscopies, high-resolution electrospray ionization mass spectrometry, and X-ray crystallography was used to examine the behavior of the compounds. It was found that **L1** and **L2** formed $[(\text{diMesbpy})\text{Cu}(\textbf{L1}\text{ or }\textbf{L2})]^{2+}$ complexes where the copper(II) diMesbpy unit was coordinated exclusively in the tridenate tripy binding site. However, when the ligands (**L1** and **L2**) were complexed with copper(I) diMesbpy units, a complex mixture was obtained. NMR and MS data indicated that a 1:1 stoichiometry of $[\text{Cu}(\text{diMesbpy})]^{+}$ and either **L1** or **L2** generated three complexes in solution, the dimetallic $[(\text{diMesbpy})_2\text{Cu}_2(\textbf{L1}\text{ or }\textbf{L2})]^{2+}$ and the monometallic $[(\text{diMesbpy})\text{Cu}(\textbf{L1}\text{ or }\textbf{L2})]^{+}$ isomers where the $[\text{Cu}(\text{diMesbpy})]^{+}$ unit is coordinated to either the bidentate or tridentate tripy binding sites of the ditopic ligands. The dimetallic $[(\text{diMesbpy})_2\text{Cu}_2(\textbf{L1}\text{ or }\textbf{L2})](\text{PF}_6)_2$ complexes were structurally characterized using X-ray crystallography. Both complexes feature a $[\text{Cu}(\text{diMesbpy})]^{+}$ coordinated to the bidentate (pytri or bpytri) pocket of the ditopic ligands (**L1** or **L2**), as expected. They also feature a second $[\text{Cu}(\text{diMesbpy})]^{+}$ coordinated to the nominally tridentate tripy binding site in a four-coordinate hypodentate κ^2-fashion. Competition experiments with model complexes showed that the binding strength of the bidentate pytri is similar to that of the κ^2-tripy ligand, leading to the lack of selectivity. The results suggest that the pytri/tripy and bpytri/tripy ligand pairs cannot be used as replacements for the more common bpy/phen-terpy partners due to the lack of selectivity in the copper(I) state.

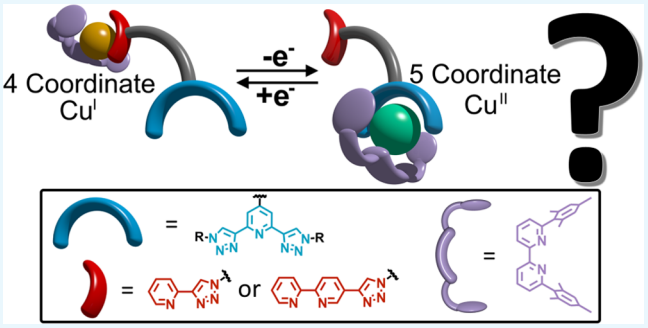

INTRODUCTION

Well-regulated molecular switches and machines are essential to life and are used extensively in all biological systems. Over the past 20 years, synthetic chemists have developed a wide range of nonbiological switches and machines. There have been some impressive devices that use mechanically interlocked architectures (MIAs, catenanes, and rotaxanes)[1−12] to generate large-scale molecular motion and/or the translocation of molecular cargo(s). Some equally sophisticated non-interlocked machine-like systems have also been generated. The vast majority of systems developed have, for the most part, exploited organic materials.[13−25] The pioneering work of Stoddart[26] and Feringa[27] in the area was recognized by their award of the 2016 Nobel prize in chemistry.

While organic systems have been used for the mainstay of molecular switches and machines, Sauvage shared the 2016 Nobel prize for his work on switchable systems that exploit transition metal ions.[28] These metal ion containing systems potentially offer useful alternative/additional properties to those provided by organic switches and machines. Coordination bonds (metal−ligand interactions) not only can be kinetically labile but also strong (thermodynamically), which can be crucial when designing dynamic/switchable systems. Additionally, metal ions potentially provide different structural

Received: September 9, 2021
Accepted: October 15, 2021
Published: October 27, 2021

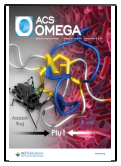

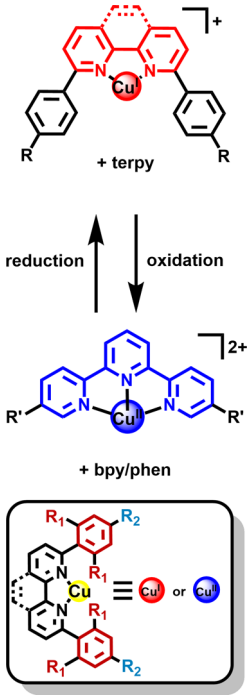

Figure 1. Generic copper(I)/copper(II) switches as developed by Sauvage and co-workers in MIAs.[40,41] The system has also been exploited in noninterlocked switching systems.[29,30]

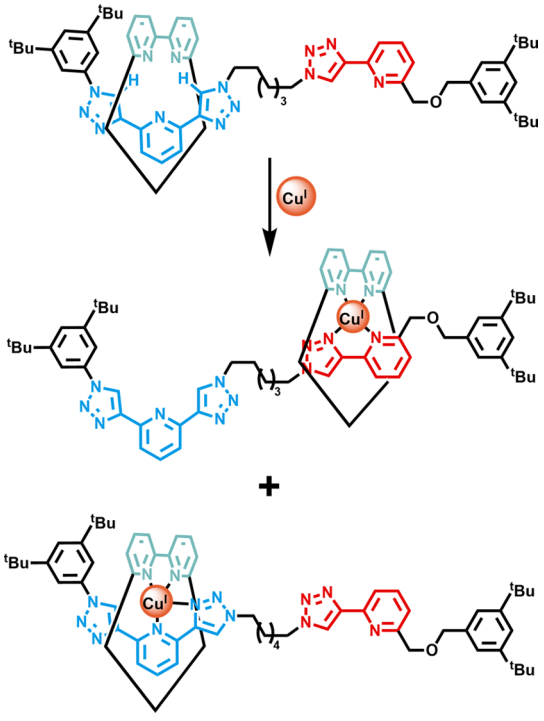

Figure 2. [2]Rotaxane copper(I)/copper(II) switch featuring pytri and tripy stations synthesized by Lewis and co-workers.[69]

motifs (geometries) when compared to carbon-based molecules and offer a range of tunable physical characteristics (e.g., redox and optical properties). Due to this, the development of molecular switches and machines that incorporate metal ions has grown exponentially in the past 10 years.[29,30] A wide range of different metal ions (Zn(II), Ag(I),[31−33] Pd(II),[34−36] and Pt(II)[37−39]) have now been examined for their use within

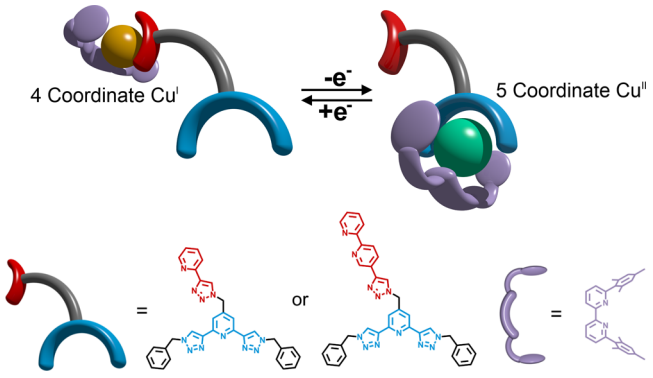

Figure 3. Targeted copper(I)/copper(II) redox switches featuring pytri (or bpytri) and tripy stations.

different machine/switch designs. However, copper ions, as first exploited by Sauvage,[28] remain the most commonly used transition metal when designing switchable systems. The enduring interest in copper(I)/copper(II)-based molecular switches is presumably due to the numerous unique properties of the copper ions. Both copper(I) and copper(II) form stable coordination complexes, and usefully, they display different coordination preferences (copper(I): four-coordinate; copper(II): higher, five-, or six-coordinate). Additionally, the different oxidation states are readily interconverted under relatively mild conditions (either chemically or electrochemically). Sauvage and co-workers developed a series of MIA systems that featured either 2,2′-bypyridine (bpy) or 1,10-phenanthroline (phen) and 2,2′;6′,2″-terpyridine (terpy) ligands and then exploited the different redox and coordination geometry preferences of the copper(I) and copper(II) ions to switch between the states (Figure 1). In an early example, Sauvage and co-workers synthesized a sophisticated [2]catenane that featured a 2,9-diphenylphenanthroline (2,9-DPphen) macrocycle interlocked to a second macrocycle that contained phen and terpy ligand sites (stations) (Figure 1).[40,41] Initially, due to the copper(I) template approach used to obtain the [2]-catenand, the 2,9-DPphen macrocycle is coordinated at the phen ligand site of the second more complex macrocycle as this satisfies the coordination geometry preference of the Cu(I) ions and generates a tetrahedrally coordinated $[Cu(phen)(2,9\text{-}DPphen)]^{+}$ co-conformer with the terpy site free. However, when the copper(I) ion is oxidized to copper(II), the harder, more highly charged copper(II) ion has different coordination geometry preferences and forms the higher, five-, or six-coordinate complex. This redox change therefore results in the translocation of the copper(II)-DPPhen macrocycle unit to the terpy site on the larger macrocycle. Cyclic voltammetry (CV) and UV−vis experiments were used to confirm that, upon oxidation, the copper containing catenand initially forms a metastable copper(II) complex in which the phen and DPphen ligands remain bound to the Cu(II) ion (i.e., $[Cu(phen)(2,9\text{-}DPphen)]^{2+}$); then, this complex slowly rearranges to the thermodynamically preferred $[Cu(2,9\text{-}DPphen)(terpy)]^{2+}$ complex, translocating the copper(II)-macrocycle unit. Reduction of that electrochemically generated complex results in the formation of a metastable $[Cu(2,9\text{-}DPphen)(terpy)]^{+}$ complex that rearranges back to the initially synthesized $[Cu(phen)(DPphen)]^{+}$ complex. The switching between the states is reversible and can be triggered chemically or electrochemically.[40,41] Using the same copper(I) and copper(II) switching process and similar ligand designs, a

https://doi.org/10.1021/acsomega.1c04977
ACS Omega 2021, 6, 30115−30129

Scheme 1. Synthesis of Ditopic Ligands L1 and L2[a]

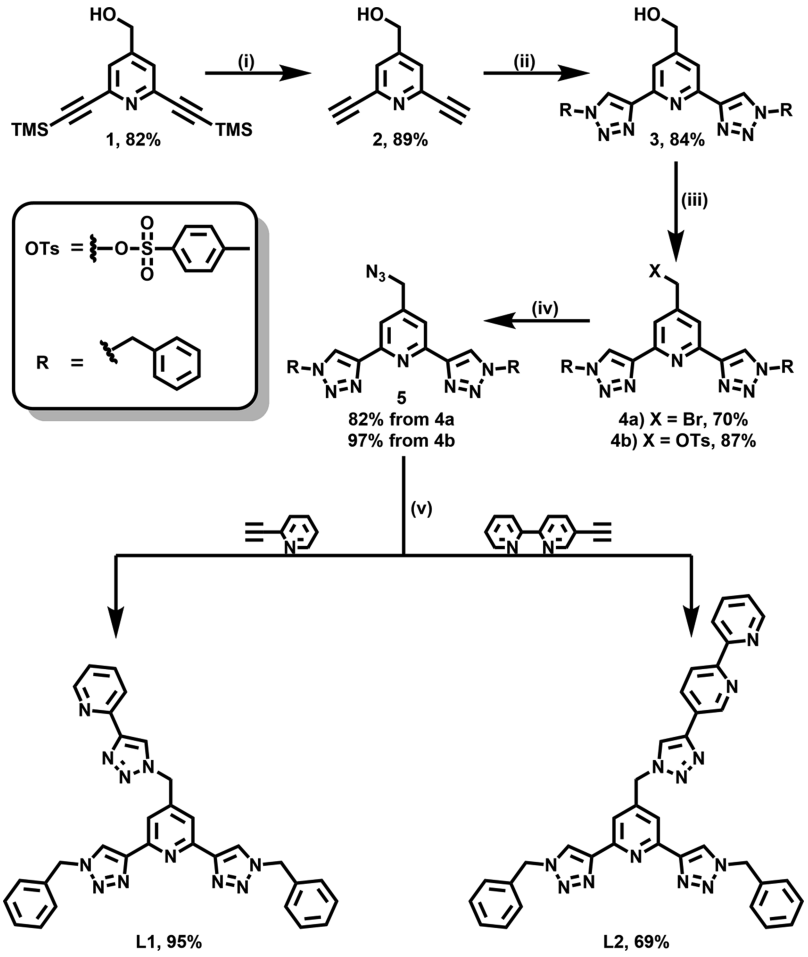

[a]Reagents and conditions: (i) Na_2CO_3, MeOH, RT, 30 mins; (ii) NaN_3, benzyl bromide, $CuSO_4{\cdot}5H_2O$, sodium L-ascorbate, 4:1 DMF/H_2O, RT, 20 h; (iii) for **4a**: CBr_4, PPh_3, DCM, RT, 19 h; for **4b**: NaOH pellets, *p*-toluenesulfonyl chloride, THF, 0 °C then RT, 2 h; (iv) NaN_3, DMF, RT, overnight; and (v) $CuSO_4{\cdot}5H_2O$, sodium L-ascorbate, 4:1 DMF/H_2O, RT, overnight.

series of mechanically interlocked copper(I)/copper(II) switches were developed by Sauvage and co-workers, including [2]rotaxane shuttles,[42,43] [2]rotaxanes that undergo macrocycle pirouetting,[44−46] and a [3]rotaxane that can "flap its wings".[47] In addition to these mechanically interlocked examples, copper(I)/copper(II) switching has also been used in noninterlocked systems. Schmittel and co-workers developed a system that could electrochemically switch the molecular cargo between two sites,[48] while Crowley and co-workers used chemical and electrochemical switching to extend and contract ferrocene-based molecular rotors.[49,50] Others have also developed copper-based electrochemical switches,[51−53] and there are copper systems where the switching is triggered chemically.[54−57] However, all the systems described above feature polypyridyl ligands (bpy, phen, and terpy) and this can complicate the synthesis of the required ligand architectures.

Recently, pyridyl 1,2,3-triazole ligands such as the bidentate 2-pyridyl-1,2,3-triazole (Rpytri) and tridentate 2,6-bis(1,2,3-triazole)pyridyl (Rtripy) moieties have emerged as replacements for bpy, phen, and terpy.[58−64] These new ligands can be readily synthesized and functionalized by exploiting the copper(I)-catalyzed azide-alkyne cycloaddition (CuAAC) "click" reaction.[65] They have also been used to develop MIAs including rotaxanes[66] and catenanes.[67,68] Lewis and co-workers have developed a [2]rotaxane that featured Rpytri and Rtripy metal binding sites as an analogue of the Sauvage-type MIA switches (Figure 2). Interestingly, when the authors added Cu(I) ions to the [2]rotaxane, a mixture containing two co-conformational isomers was obtained.[69] The major co-conformation was shown to be the expected four-coordinate copper(I) complex featuring the metal ion ligated to the bpy macrocycle and the Rpytri station. In the second co-conformer, the copper(I)-bpy macrocycle unit is bound to the nominally tridentate Rtripy station. However, the authors proposed that the Rtripy unit was hypodentate[70,71] and acting as the bidentate (κ^2) ligand rather than the expected tridentate (κ^3) coordination mode (Figure 2).

Herein, inspired by the work of Lewis and co-workers,[69] we report the synthesis of two new ditopic ligands (**L1** and **L2**): one features 2-(1-benzyl-1*H*-1,2,3-triazol-4-yl)pyridine (pytri) and 2,6-bis[(4-phenyl-1*H*-1,2,3-triazol-1-yl)methyl]pyridine (tripy) binding sites and the other features 1-benzyl-4-(2,2′-bipyridin-5-yl)-1*H*-1,2,3-triazole (bpytri) and tripy units. In an effort to develop a new metal-based switching system, the copper(I) and copper(II) coordination chemistries of the ligands were examined (Figure 3). The complexes were characterized using a range of techniques (^{1}H and ^{13}C nuclear magnetic resonance (NMR) and electronic (UV−vis) spectroscopy, high-resolution electrospray ionization mass spec-

https://doi.org/10.1021/acsomega.1c04977
ACS Omega 2021, 6, 30115−30129

trometry (HRESI-MS), and X-ray crystallography). Additionally, a series of model complexes were examined to provide further insight into the switching behavior of the systems.

RESULTS AND DISCUSSION

Model Copper Complexes. Prior to synthesizing the ditopic ligands (**L1** and **L2**; Scheme 1), three model copper complexes were generated (Figure 4 and the Supporting Information) to confirm that the different binding pockets would coordinate the relevant copper ions (Cu(I) for the bidentate ligands or Cu(II) for the tridentate ligand) in the expected manner. To synthesize the heteroleptic copper(I) complexes, 6,6′-dimesityl-2,2′-bipyridine (diMesbpy, 1 equiv)[72] and $[Cu(MeCN)_4](PF_6)$ (1 equiv) were combined in acetone to form the $[Cu(MeCN)_2(diMesbpy)](PF_6)$ intermediate.[50,73] Then, either 2-(1-benzyl-1*H*-1,2,3-triazol-4-yl)pyridine (pytri)[74] or 1-benzyl-4-(2,2′-bipyridin-5-yl)-1*H*-1,2,3-triazole (bpytri)[75] (1 equiv) was added to generate dark red solutions from which orange/red crystals could be obtained (Supporting Information). The heteroleptic Cu(II) complex was synthesized by stirring $CuCl_2$ (1 equiv) and $AgPF_6$ in acetone to extract the chloride ions and generate the solvated Cu(II) complex in solution. Then, the diMesbpy (1 equiv) and 2,6-bis[(4-phenyl-1*H*-1,2,3-triazol-1-yl)methyl]-pyridine (tripy)[74] ligands were added sequentially, generating a blue solution. The copper complexes were characterized using a combination of ^1H and ^{13}C NMR and UV−vis spectroscopies, HRESI-MS, and elemental analysis. Additionally, the molecular structures of all three complexes were confirmed using X-ray crystallography (Supporting Information, Figures S52 and S53 and Figure 4).

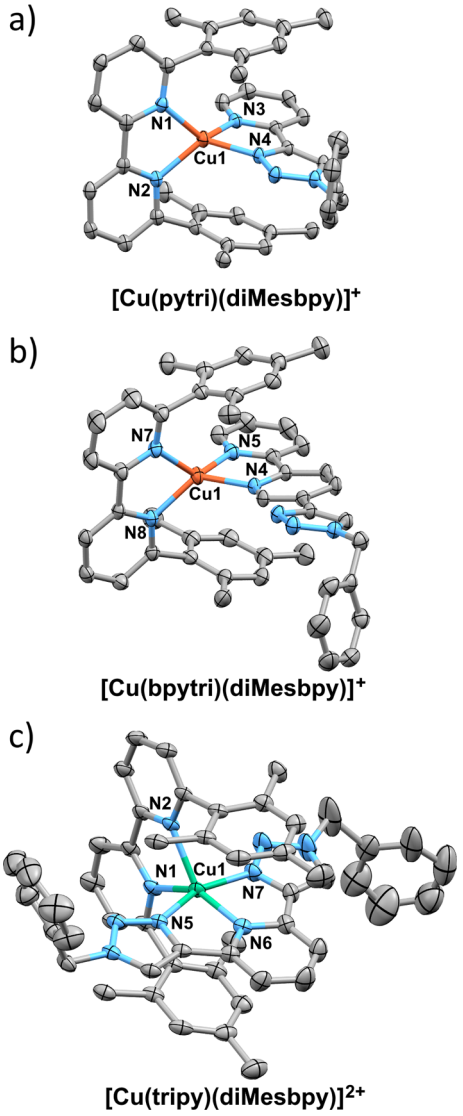

Figure 4. ORTEP diagrams of the molecular structures of (a) $[Cu(pytri)(diMesbpy)](PF_6)$, (b) $[Cu(bpytri)(diMesbpy)](PF_6)$, and (c) $[Cu(tripy)(diMesbpy)](PF_6)_2$. Selected bond lengths (Å) and angles (°): (a) Cu1-N1 2.016(2), Cu1-N2 2.039(2), Cu1-N3 2.036(2), Cu1-N4 2.031(2), N1-Cu1-N4 127.89(9), and N2-Cu1-N3 128.2(2); (b) Cu1-N4 2.045(2), Cu1-N5 2.009(3), Cu1-N6 2.021(3), Cu1-N7 2.041(2), N5-Cu1-N6 129.2(1), and N5-Cu1-N7 131.5(1); (c) Cu1-N1 2.068(2), Cu1-N2 2.109(2), Cu1-N5 2.010(3), Cu1-N6 1.979(3), Cu1-N7 2.019(3), N1-Cu1-N6 144.4(1), and N5-Cu1-N7 158.3(1). Thermal ellipsoids shown at the 50% probability level. Counteranions, solvent molecules, and hydrogen atoms are omitted for clarity. Colors: copper(I), orange; copper(II), green; nitrogen, blue; carbon, gray.

Previously, we have reported the molecular structure of the heteroleptic Cu(I) complex, $[Cu(pytri)(diMesbpy)](PF_6)$.[73] As expected, the complex displayed a four-coordinate distorted tetrahedral geometry (τ_4[76] = 0.73).[73] Similar to $[Cu(pytri)(diMesbpy)](PF_6)$, the $[Cu(bpytri)(diMesbpy)](PF_6)$ complex also shows a distorted tetrahedral geometry (τ_4 = 0.70). The Cu(II) complex $[Cu(tripy)(diMesbpy)](PF_6)_2$ adopts the expected five-coordinate geometry; however, while the complex appears to be trigonal bipyramidal, a τ_5 parameter[77] of 0.23 indicates that it is much closer to the square-based pyramidal geometry. This is still significantly more trigonal bipyramidal than the related $[Cu(tripy)Cl_2]$ complex (τ_5 = 0.05)[74] and is similar to the analogous $[Cu(terpy)(diMesbpy)](PF_6)_2$ complex (τ_5 = 0.29).[49,50]

Ditopic Ligand Synthesis. Assured that the different binding pockets (pytri, bpytri, and tripy) could coordinate the copper(I/II) diMesbpy units in the desired manner, two ditopic potential switch ligands were synthesized (Scheme 1 and the Supporting Information).

The trimethylsilyl (TMS)-protected pyridine **1** was synthesized using a previously reported method;[78] then, the TMS protecting groups were removed using Na_2CO_3 in methanol to provide the dialkyne **2**. This was then reacted with sodium azide, benzyl bromide, copper(II) sulfate, and sodium L-ascorbate in DMF/water (standard *in situ* azide-formation "click" conditions),[74] forming the tridentate, tripy, binding pocket, **3**. Initially, **3** was converted into the bromo analogue (**4a**, 70%) using the Appel reaction (PPh_3, CBr_4). However, the triphenylphosphine oxide byproduct proved difficult to remove from **4a**. Therefore, **3** was converted to **4b** (87%) using 4-toluenesulfonyl chloride. Either **4a** or **4b** could then be reacted with sodium azide in DMF solution to give **5** (82 or 97%). Finally, **5** was combined with either 2-ethynylpyridine or 5-ethynyl-2,2′-bipyridine using click reaction conditions to provide the two ditopic ligands **L1** and **L2**, respectively, in moderate-to-good yields (69 or 95%, respectively). All the new compounds were characterized using ^1H and ^{13}C NMR spectroscopies, HRESI-MS, and elemental analysis (Supporting Information).

Cu(II) Complexes. Having successfully synthesized the two ditopic ligands, their coordination properties with Cu(II) were explored. At first, formation of the [Cu(**L1**)(diMesbpy)]-

https://doi.org/10.1021/acsomega.1c04977
ACS Omega 2021, 6, 30115−30129

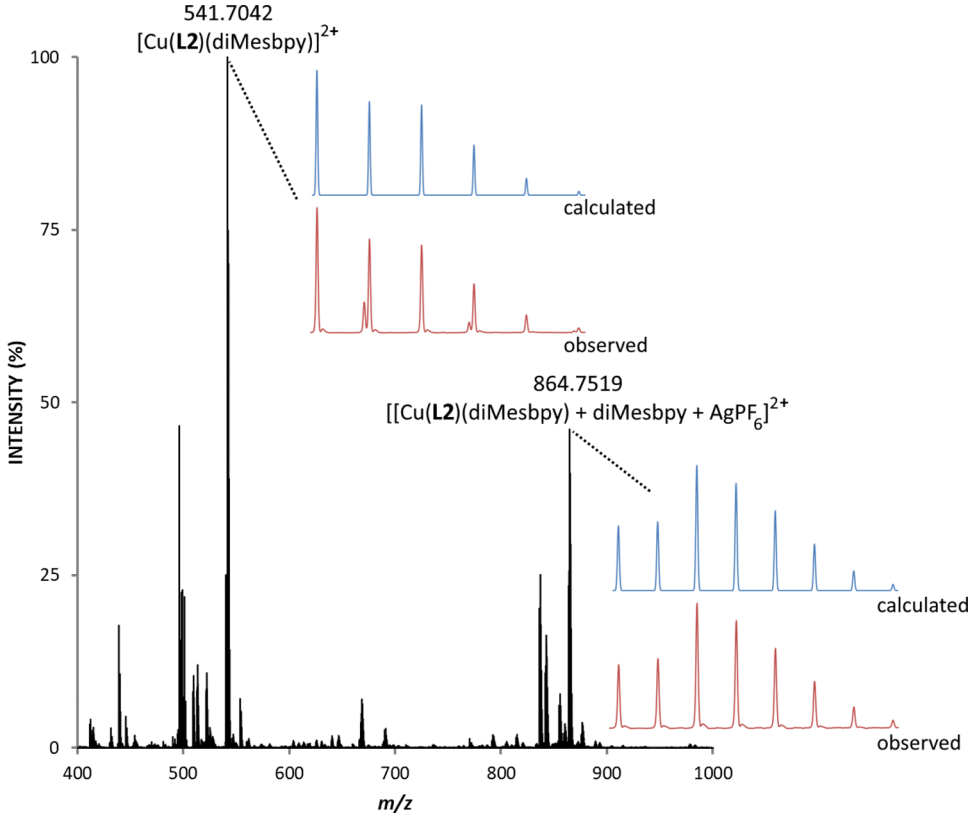

Figure 5. Partial HRESI-MS (acetone/MeOH) of $[Cu(\mathbf{L2})(diMesbpy)](PF_6)_2$ synthesized using $CuCl_2$ and $AgPF_6$.

Scheme 2. Synthesis of $[Cu(L1)(diMesbpy)](PF_6)_2$ and $[Cu(L2)(diMesbpy)](PF_6)_2$[a]

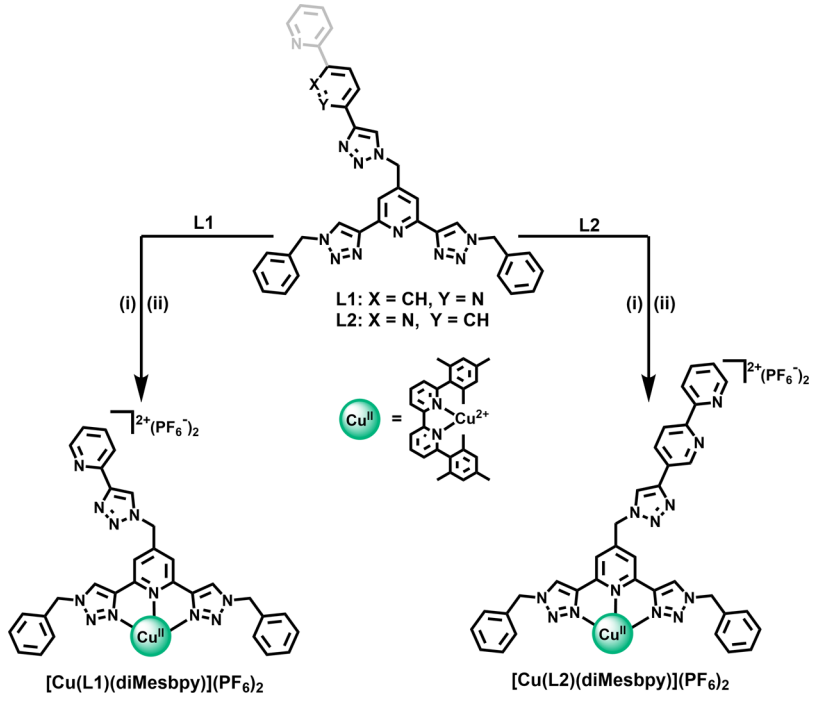

[a]Reagents and conditions: (i) $Cu(NO_3)_2{\cdot}3H_2O$, diMesbpy, 1:1:1 acetone:MeOH:MeCN, RT, 1.5 h; (ii) sat. NH_4PF_6 (aq), 85 °C, 1 h.

$(PF_6)_2$ and $[Cu(\mathbf{L2})(diMesbpy)](PF_6)_2$ complexes was attempted exploiting the procedure used to generate the $[Cu(tripy)(diMesbpy)](PF_6)_2$ model complex (*vide supra*). $CuCl_2$ was stirred in acetone solution with $AgPF_6$ to extract the chloride ligands leaving the solvated Cu(II) ion. Once the AgCl had been removed by filtration through Celite, the solution of solvated Cu(II) ions was added to diMesbpy, forming a green solution of the solvated $[Cu(diMesbpy)]^{2+}$ intermediate. To this, solution was added **L1** or **L2** forming either a blue or brown/green solution, respectively. Sub-

https://doi.org/10.1021/acsomega.1c04977
ACS Omega 2021, 6, 30115−30129

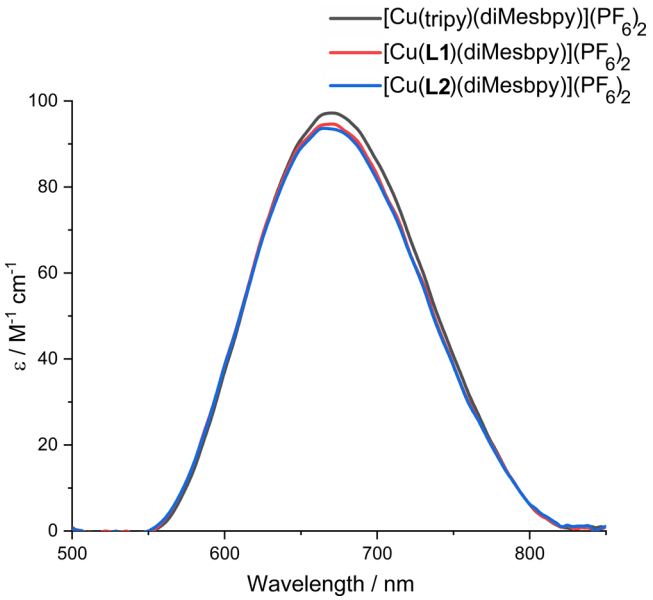

Figure 6. UV−vis spectra of the Cu(II) complexes in MeCN at 298 K.

sequent addition of diethyl ether led to the precipitation of blue/green solids (Supporting Information). ^{1}H NMR spectroscopy of the complexes in d_6-acetone solution gave broad featureless spectra consistent with the formation of paramagnetic Cu(II) species (Supporting Information, Figure S43). HRESI-MS data were consistent with the formation of the desired complexes with intense peaks corresponding to the dicationic $[Cu(\mathbf{L1})(diMesbpy)]^{2+}$ (m/z = 503.1902) and $[Cu(\mathbf{L2})(diMesbpy)]^{2+}$ (m/z = 541.7042) species being observed. However, the mass spectrum of $[Cu(\mathbf{L2})(diMesbpy)](PF_6)_2$ displayed a second peak at m/z = 864.7519, which could be assigned as $[[Cu(\mathbf{L2})(diMesbpy)] + diMesbpy + AgPF_6]^{2+}$, suggesting that $AgPF_6$ was still present (Figure 5 and the Supporting Information). This was further corroborated by the elemental analysis of the complexes. A similar behavior was also found to occur with the Cu(II) complex of **L1**.

Small X-ray quality crystals were obtained from the vapor diffusion of diisopropyl ether into an acetonitrile solution of the isolated $[Cu(\mathbf{L1})(diMesbpy)](PF_6)_2$ complex. While the diffraction and the resulting data obtained from the crystals were modest, the structure of the complex and the bond connectivity could be ascertained (Supporting Information, Figures S41 and S54). As expected, the $[Cu(diMesbpy)]^{2+}$ unit was shown to be coordinated in the tripy pocket of **L1**. However, the pytri pocket was coordinated to a Ag(I) ion generating a heterotrimetallic complex $[\{(diMesbpy)Cu(\mathbf{L1})\}_2Ag](PF_6)_3$, consistent with the elemental analysis and ESI-MS data (Supporting Information). Given that the Ag(I) ion could be a source of competition for Cu(I) during any subsequent copper(I)/(II) switching, an alternate route to the Cu(II) complexes, a new method that avoided the use of Ag(I), was targeted. To this end, diMesbpy was added to an acetone solution of $Cu(NO_3)_2{\cdot}3H_2O$ followed by either **L1** or **L2** (Scheme 2). After stirring for 1 h, the resulting blue solutions were treated with a saturated aqueous solution of NH_4PF_6, resulting in blue precipitates that were collected by vacuum filtration. After washing with copious amounts of water, the solids were redissolved in acetonitrile and precipitated with diethyl ether providing the desired complexes as pale blue powders in good yield (76% for $[Cu(\mathbf{L1})$-

Scheme 3. Synthesis of $[Cu_2(\mathbf{L1})(diMesbpy)_2](PF_6)_2$ and $[Cu_2(\mathbf{L2})(diMesbpy)_2](PF_6)_2$[a]

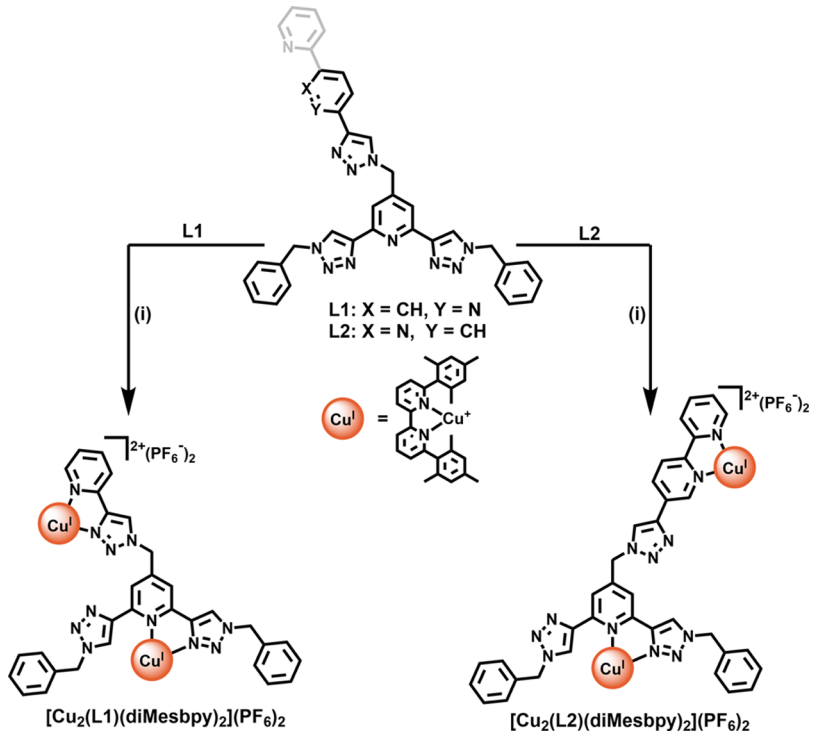

[a]Reagents and conditions: (i) $[Cu(MeCN)_4](PF_6)$, diMesbpy, acetone, RT, 1.5 h.

https://doi.org/10.1021/acsomega.1c04977
ACS Omega 2021, 6, 30115−30129

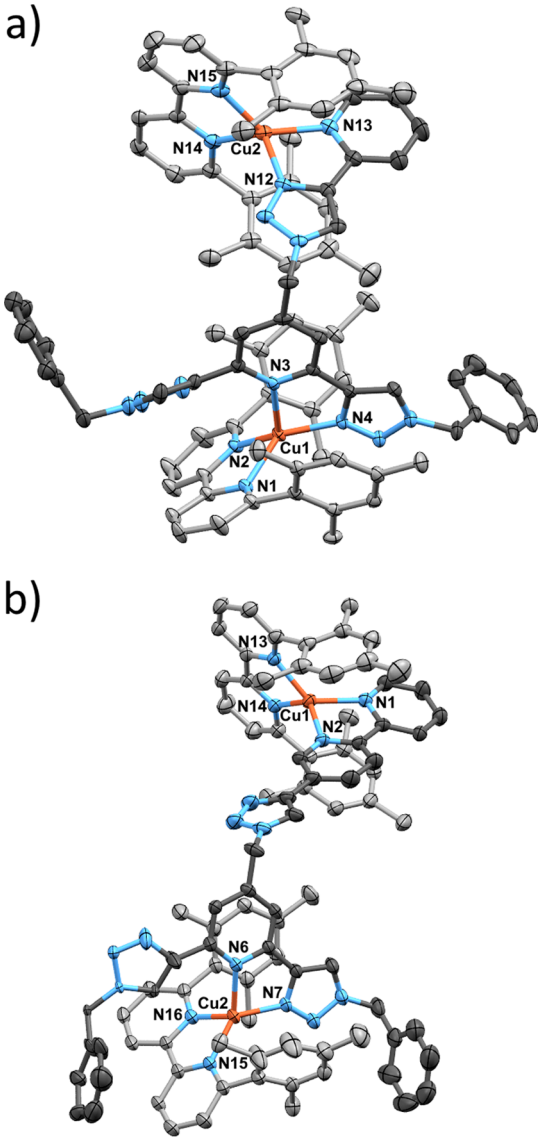

Figure 7. Molecular structures of $[Cu_2(\mathbf{L1})(diMesbpy)_2](PF_6)_2$ and $[Cu_2(\mathbf{L2})(diMesbpy)_2](PF_6)_2$. (a) $[Cu_2(\mathbf{L1})(diMesbpy)_2](PF_6)_2$ (P isomer) present in the asymmetric unit. Selected bond lengths (Å) and angles (°): Cu1-N1 2.067(2), Cu1-N2 2.004(2), Cu1-N3 2.159(2), Cu1-N4 1.978(2), Cu2-N12 2.017(3), Cu2-N13 2.032(2), Cu2-N14 2.027(2), Cu2-N15 2.016(3), N2-Cu1-N4 140.85(9), N2-Cu1-N3 125.16(9), N13-Cu2-N14 131.7(1), and N13-Cu2-N15 130.6(1); (b) $[Cu_2(\mathbf{L2})(diMesbpy)_2](PF_6)_2$ obtained from the 1:1 mixture of $[Cu(diMesbpy)]^+$:**L2**. Selected bond lengths (Å) and angles (°): Cu1-N1 2.032(3), Cu1-N2 2.048(2), Cu1-N13 2.038(2), Cu1-N14 2.041(3), Cu2-N6 2.125(2), Cu2-N7 1.965(2), Cu2-N15 1.999(2), Cu2-N16 2.045(3), N1-Cu1-N13 128.91(9), N2-Cu1-N14 128.76(9), N7-Cu2-N15 130.5(1), and N6-Cu2-N15 129.92(1). Thermal ellipsoids shown at the 50% probability level. Counteranions, solvent molecules, and hydrogen atoms were omitted for clarity. Colors: copper(I), orange; nitrogen, blue; carbon, gray/dark gray.

$(diMesbpy)](PF_6)_2$ and 78% for $[Cu(\mathbf{L2})(diMesbpy)](PF_6)_2$).

HRESI-MS data was consistent with the formation of the copper(II) complexes. Peaks were observed at m/z = 503.1884 and 541.7039, respectively, corresponding to the dicationic species $[Cu(\mathbf{L1})(diMesbpy)]^{2+}$ and $[Cu(\mathbf{L2})(diMesbpy)]^{2+}$. Elemental analysis was also consistent with the formation of the monometallic copper(II) complexes $[Cu(\mathbf{L1})(diMesbpy)](PF_6)_2$ and $[Cu(\mathbf{L2})(diMesbpy)](PF_6)_2$. Disappointingly, despite extensive efforts, attempts to grow crystals of the two complexes proved to be unsuccessful. UV−visible absorption spectrophotometry was used to confirm that the $[Cu(diMesbpy)]^{2+}$ unit was bound within the tridentate tripy pocket of the **L1** or **L2** ligands, as opposed to the bidentate pytri or bpytri. The UV−vis spectra of the model $[Cu(tripy)(diMesbpy)](PF_6)_2$ complex, $[Cu(\mathbf{L1})(diMesbpy)](PF_6)_2$, and $[Cu(\mathbf{L2})(diMesbpy)](PF_6)_2$ were collected in acetonitrile. As shown in Figure 6, all the complexes show a weak absorption (ε = 90−100 M^{-1} cm^{-1}) around 670 nm, typical of a d−d transition, suggesting that the Cu(II) ion is bound in a similar fashion in each of the complexes (i.e., within a tripy tridentate pocket).

Cu(I) Complexes. Having confirmed that **L1** and **L2** could form monometallic copper(II) complexes with the $[Cu(diMesbpy)]^{2+}$ unit bound within the tridentate tripy pocket, we next examined the synthesis of the monometallic Cu(I) complexes. $[Cu(MeCN)_4](PF_6)$ and diMesbpy were stirred in acetone to form the $[Cu(diMesbpy)(MeCN)_2](PF_6)$ intermediate, to which after filtering to remove any Cu(II) species was added either **L1** or **L2**. After stirring, a petroleum ether/diethyl ether (3:1) solution was added producing orange/red precipitates that were isolated by vacuum filtration. HRESI-MS data of the isolated Cu(I) products displayed large peaks at m/z = 1006.3812 and 1083.4064, consistent with the presence of the monocationic species $[Cu(\mathbf{L1})(diMesbpy)]^+$ or $[Cu(\mathbf{L2})(diMesbpy)]^+$, respectively. These suggested that complexes with the desired 1:1 stoichiometry of $[Cu(diMesbpy)]^+$ to the ditopic ligand were formed. However, the HRESI-MS data of the isolated material also showed an almost equal intensity peak at m/z = 770.2805 (for **L2**) corresponding to a dicationic species with a two-to-one stoichiometry of $[Cu(diMesbpy)]^+$ to **L2** (i.e., $[Cu_2(\mathbf{L2})(diMesbpy)_2]^{2+}$). A similar species, $[Cu_2(\mathbf{L1})(diMesbpy)_2]^{2+}$, was observed for the product of complexation with **L1** at m/z = 731.7679. This suggested that the isolated materials may be a mixture of mono- and dimetallic complexes. The ^{1}H NMR spectra of the isolated Cu(I) **L1** or **L2** products also suggested the formation of a mixture of species rather than just the desired complexes ($[Cu(\mathbf{L1})(diMesbpy)](PF_6)$ and $[Cu(\mathbf{L2})(diMesbpy)](PF_6)$). In contrast to the copper(I) model complexes (*vide supra*), the ^{1}H NMR spectra of the copper(I) diMesbpy complexes of **L1** and **L2** were broad and relatively undefined (Supporting Information). The broad nature of the NMR spectrum could potentially be caused by three factors: (i) the presence of paramagnetic Cu(II) ions, (ii) exchange of the $[Cu(diMesbpy)]^+$ units between the bidentate and tridentate sites of **L1**/**L2**, and (iii) a mixture of species in solution. Sodium ascorbate (a reducing agent) was added to the mixtures, and the ^{1}H NMR spectra were reobtained; no change in the spectra was observed ruling out the presence of Cu(II) species as the cause of the broadness. To examine if the exchange of the $[Cu(diMesbpy)]^+$ units between the bidentate and tridentate sites of **L1**/**L2** was the cause of the broadened spectra, we synthesized coordinatively saturated diCu(I) complexes of **L1** and **L2** (Scheme 3). Using the same conditions (*vide supra*) but adding two equivalents of diMesbpy and $[Cu(MeCN)_4](PF_6)$ to the ditopic ligands (either **L1** or **L2**) resulted in the formation of the diCu(I) complexes (Scheme 3). The complexes were isolated as orange powders in good yields (94% for $[Cu_2(\mathbf{L1})(diMesbpy)_2]$-

https://doi.org/10.1021/acsomega.1c04977
ACS Omega 2021, 6, 30115−30129

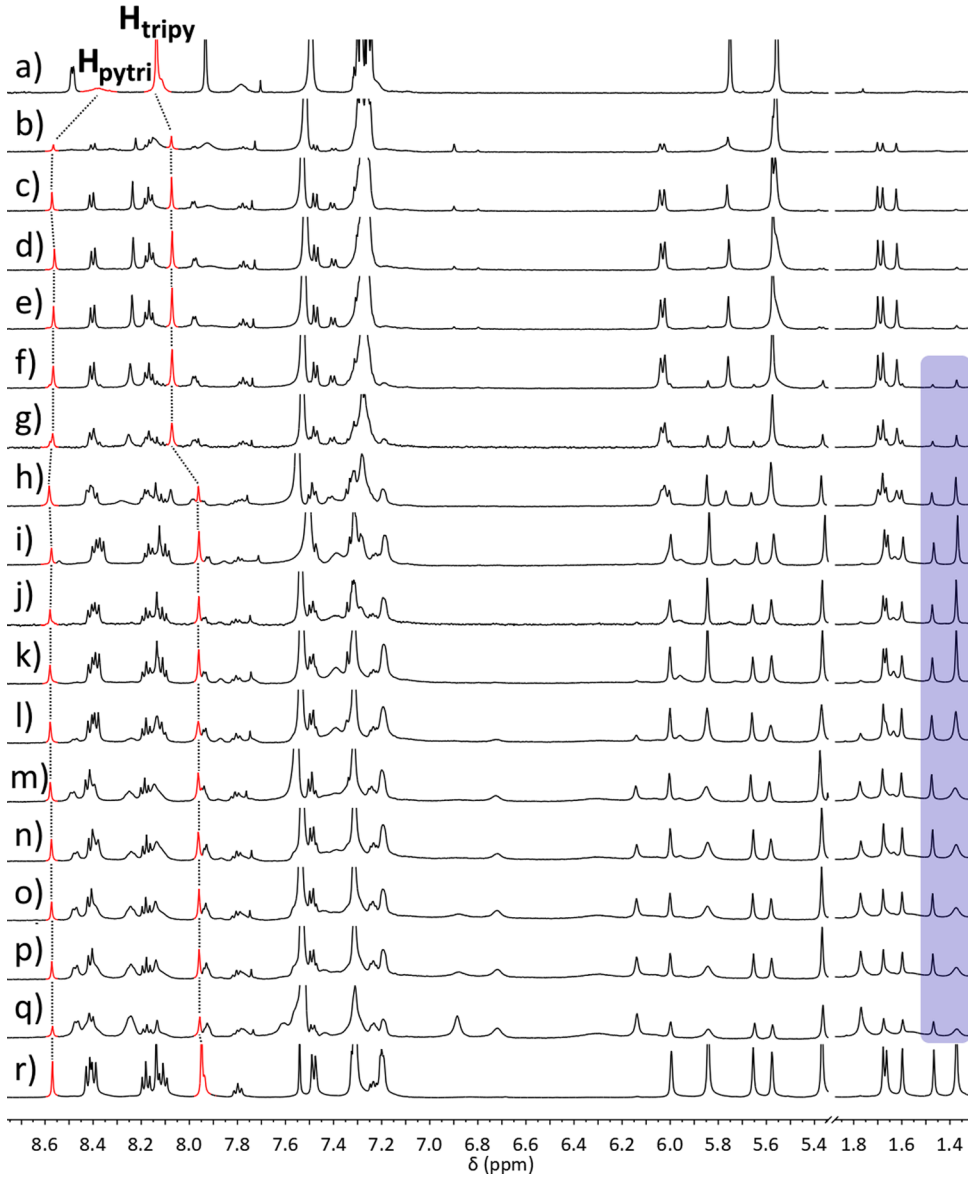

Figure 8. Partial ^{1}H NMR (500 MHz, 2:1 $CDCl_3$:d_6-acetone, 298 K) spectra of the titration of $[Cu(diMesbpy)(MeCN)_2](PF_6)$ into **L1** at (a) 0 equiv of $[Cu(diMesbpy)(MeCN)_2](PF_6)$, (b) 0.2 equiv, (c) 0.4 equiv, (d) 0.5 equiv, (e) 0.6 equiv, (f) 0.8 equiv, (g) 1 equiv, (h) 1.2 equiv, (i) 1.4 equiv, (j) 1.5 equiv, (k) 1.6 equiv, (l) 1.8 equiv, (m) 2 equiv, (n) 2.2 equiv, (o) 2.4 equiv, (p) 2.5 equiv, (q) 3 equiv, and (r) independently isolated $[Cu_2(\mathbf{L1})(diMesbpy)_2](PF_6)_2$.

$(PF_6)_2$ and 81% for $[Cu_2(\mathbf{L2})(diMesbpy)_2](PF_6)_2$) and were characterized using 1D and 2D NMR spectroscopies, HRESI-MS, and elemental analysis (Supporting Information). The ^{1}H NMR spectra of the diCu(I) complexes of **L1** and **L2** were sharper and well defined (Supporting Information, Figure S46), providing strong support for the postulate where the broadened spectra observed for the 1:1 metal:ligand ratios are because of the exchange between the two binding sites of the ditopic ligands. Comparison of the ^{1}H NMR spectra obtained for the diCu(I) complexes with the spectra obtained on the 1:1 Cu(I):**L1**/**L2** ratio also indicated that the diCu(I) complexes were present in solution at the lower metal-to-ligand ratio (Supporting Information). Overall, the NMR and HRESI-MS data suggest that, at a 1:1 ratio of Cu(I):**L1**/**L2**, both mono- and dicopper(I) complexes are present.

To gain further insight into the molecular structures of the copper(I) complexes, mixtures (1:1 and 2:1 ratios) of $[Cu(diMesbpy)]^+$:**L1** or **L2** were prepared in acetonitrile and vapor-diffused with diethyl ether. Red X-ray quality crystals were obtained for **L1** from the solution with a 2:1 copper:ligand ratio. Conversely, the 1:1 $[Cu(diMesbpy)]^+$:**L2** reaction mixture provided red crystals of the **L2** copper(I) complex suitable for X-ray diffraction. Interestingly, despite the different starting ratios, the crystals contained the dicopper(I) complexes $[Cu_2(\mathbf{L1})(diMesbpy)_2](PF_6)_2$ and $[Cu_2(\mathbf{L2})(diMesbpy)_2](PF_6)_2$ (Figure 7 and the Supporting Information, Figures S55 and S56).

The molecular structure of $[Cu_2(\mathbf{L1})(diMesbpy)_2](PF_6)_2$ was solved in the triclinic $P\bar{1}$ space group and featured two crystallographically independent $[Cu_2(\mathbf{L1})(diMesbpy)_2]^{2+}$ units, namely, P and M helices, along with four PF_6^- anions and an acetonitrile molecule in the unit cell (Supporting Information, Figure S55). The molecular structure of $[Cu_2(\mathbf{L2})(diMesbpy)_2](PF_6)_2$ was also solved in the triclinic

https://doi.org/10.1021/acsomega.1c04977
ACS Omega 2021, 6, 30115−30129

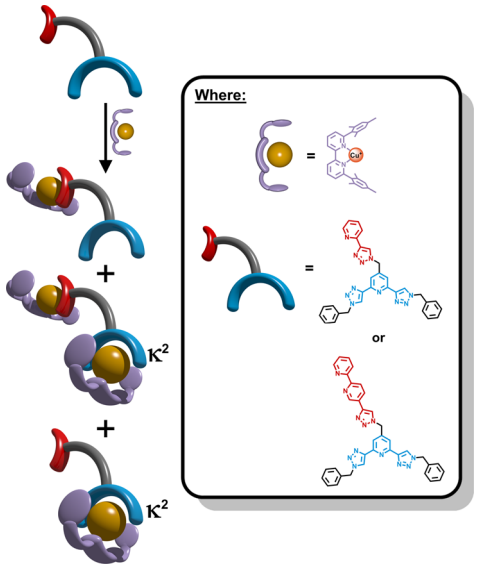

Figure 9. Cartoon representation of the different species present in solution when $[Cu(diMesbpy)]^+$ is complexed with the ditopic ligands **L1** and **L2**.

$P\bar{1}$ space group; however, the unit cell contained one $[Cu_2(\mathbf{L2})(diMesbpy)_2]^{2+}$cation, two PF_6^- anions, and an acetonitrile molecule (Supporting Information, Figure S56). In both structures, as expected, a $[Cu(diMesbpy)]^+$ unit was coordinated to the bidentate pocket of the ditopic ligands (either pytri for **L1** or bpytri for **L2**; Figure 7). The $[Cu(diMesbpy)(N{-}N)]^+$ units (where N−N = pytri or bpytri) both display four-coordinate distorted tetrahedral geometries (τ_4 = 0.73 or 0.71), and the bond metrics are very similar to those observed in the analogous model complexes $[Cu(pytri)(diMesbpy)](PF_6)$ and $[Cu(bpytri)(diMesbpy)](PF_6)$ (*vide supra*).

In both the dicopper(I) complexes, a second $[Cu(diMesbpy)]^+$ unit was coordinated to the nominally tridentate tripy pocket (Figure 7 and the Supporting Information, Figures S55 and S56). However, the tripy units are not acting as tridentate donor units. Instead, they are displaying hypodentate[70,71] behavior. One of the triazole arms is rotated away from the copper(I) ions (by between 90 and 180°), resulting in a bidentate pytri-like chelating pocket (i.e., κ^2-tripy coordination mode; Figure 7 and the Supporting Information, Figures S55 and S56). Therefore, both the $[Cu(diMesbpy)(tripy)]^+$ motifs in the **L1** and **L2** dicopper(I) complexes display four-coordinate distorted tetrahedral geometries (τ_4 = 0.67, 0.69, and 0.71 in the crystallographically independent units) and the tripy units exhibit hypodentate κ^2-coordination. The hypodentate κ^2-coordination mode of the tripy units is also reminiscent of the behavior observed by Lewis and co-workers[69] in their triazole-based rotaxane system (Figure 2). However, in their unsymmetrical tripy example, the two triazole arms would have different donor strengths, whereas in the current symmetrical systems, the donor strengths of the two triazole arms are identical. More recently, during the course of our work, Goldup and co-workers have obtained the molecular structure of a copper(I) [2]rotaxane complex that featured bpy and tripy metal binding pockets. They found that the copper(I) ion adopted a four-coordinate distorted tetrahedral geometry (τ_4 = 0.66) with a hypodentate κ^2-coordination mode of the tripy unit similar to what we have observed. However, interestingly, in their copper(I) [2]-rotaxane complex, the triazole that is not coordinated has not rotated away from the copper(I) ion, the nitrogen atom of the 1,2,3-triazole arm still points toward the copper(I), but the Cu−N distance (2.854(2) Å) is too long to be a bonding interaction.[66] The results suggest, somewhat surprisingly, that tripy ligands are able to readily adopt a hypodentate κ^2-coordination rather than the expected, and more common, κ^3-coordination.[63]

^{1}H NMR Titration Experiments. To gain more information about the dynamics and speciation of the Cu(I) diMesbpy complexes of the ditopic ligands (**L1** and **L2**), ^{1}H NMR titration experiments were carried out. Increasing equivalents of $[Cu(diMesbpy)(MeCN)_2](PF_6)$ (0−3 equiv) were added to either **L1** (1.1 mM) or **L2** (0.5 mM) in 2:1 $CDCl_3$:d_6-acetone, and the species formed were monitored by ^{1}H NMR spectroscopy (Figure 8 and the Supporting Information, Figure S48).

The data for **L1** are shown in Figure 8 (the analogous data for **L2** are in the Supporting Information, Figure S48). As soon as $[Cu(diMesbpy)(MeCN)_2](PF_6)$ (0.2 equiv) was added, the positions of the two unique triazole protons (H_{pyrtri} for bidentate triazole and H_{tripy} for tridentate triazole) experience shifts indicative of complexation to a $[Cu(diMesbpy)]^+$ unit. Interestingly, only three methyl resonances are observed for the $[Cu(diMesbpy)]^+$, suggesting that the $[Cu(diMesbpy)]^+$ unit is coordinated and exchanging between the pytri (or bpytri) and κ^2-tripy binding sites. There are several other broad resonances that support that postulate. At 0.8 equiv of $[Cu(diMesbpy)(MeCN)_2](PF_6)$, new methyl peaks begin to appear (blue box) and grow larger in the presence of 1−2 equiv of $[Cu(diMesbpy)(MeCN)_2](PF_6)$. The chemical shifts of those methyl resonances correspond well with the methyl signal observed for the isolated dicopper(I) complexes, suggesting that those mixtures of $[Cu(diMesbpy)(MeCN)_2](PF_6)$ and the ditopic ligands (**L1** or **L2**) contain both the mono- and dicopper(I) complexes. Additionally, at 1.2 equiv of $[Cu(diMesbpy)(MeCN)_2](PF_6)$, the H_{tripy} peak from the tridentate triazole undergoes another shift, suggesting that the dicopper(I) complex is now dominating the observed spectrum. Past 2 equiv of $[Cu(diMesbpy)(MeCN)_2](PF_6)$, the spectra are dominated by the dicopper(I) complexes and free $[Cu(diMesbpy)(MeCN)_2](PF_6)$, suggesting that both binding pockets of the ligands (**L1** and **L2**) are saturated with copper(I) diMesbpy units. The data suggest that, below 0.8 equiv of $[Cu(diMesbpy)(MeCN)_2](PF_6)$, the solution contains a mixture of the two monocopper(I) complexes where the $[Cu(diMesbpy)]^+$ unit is coordinated to either the pytri (bpytri) or the tripy (with a κ^2-coordination mode). Between 0.8 and 1.8 equiv of $[Cu(diMesbpy)(MeCN)_2](PF_6)$, it is likely that there are three species, namely, two monometallic complexes and the dimetallic complex where a $[Cu(diMesbpy)]^+$ unit is coordinated in both the bidentate and κ^2-tripy pockets (i.e., $[Cu_2(\mathbf{L1}/\mathbf{L2})(diMesbpy)_2](PF_6)_2$) (Figure 9). Unfortunately, due to the broadness and complexity of the spectra produced, the amounts of each of the different copper(I) complexes in solution could not be readily determined. However, if all these species are present, then it indicates that the binding strengths of the bidentate (pytri/bpytri) and κ^2-tripy pockets are very similar. This is not surprising in the case of **L1** where the bidentate pytri and κ^2-tripy pockets both form pyridyl triazole ligands. However, it is slightly more surprising for **L2** where the bidentate site is a bpy

https://doi.org/10.1021/acsomega.1c04977
ACS Omega 2021, 6, 30115−30129

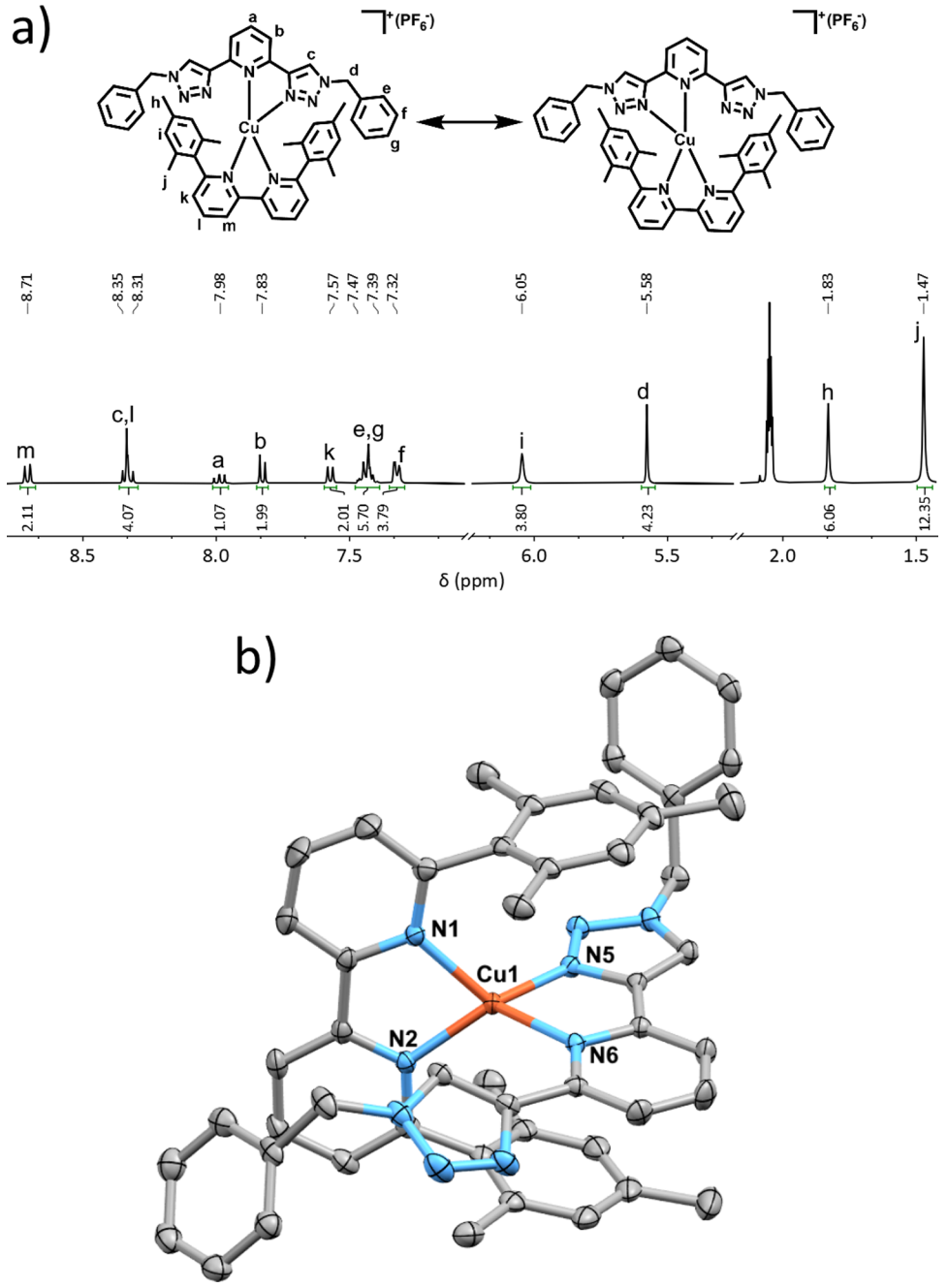

Figure 10. (a) Partial ^{1}H NMR (400 MHz, d_6-acetone, 298 K) spectra of [Cu(κ^2-tripy)(diMesbpy)](PF$_6$) and fluxional process that generates the symmetric ^{1}H NMR spectrum. (b) Molecular structure of [Cu(κ^2-tripy)(diMesbpy)](PF$_6$). Selected bond lengths (Å) and angles (°): Cu1-N1 2.025(1), Cu1-N2 2.008(1), Cu1-N5 1.993(1), Cu1-N6 2.044(1), N1-Cu1-N6 126.82(5), and N2-Cu1-N5 128.14(5). Thermal ellipsoids shown at the 50% probability level. Counteranions, solvent molecules, and hydrogen atoms were omitted for clarity. Colors: copper(I), orange; nitrogen, blue; carbon, gray.

moiety as it has been shown previously that bpy is a much stronger donor than pytri moieties[79] and thus should bind a metal ion more strongly. However, the observed data suggest that the tripy metal binding site competes with the bpytri site for the [Cu(diMesbpy)]$^+$ unit.

Competition Studies with Model Complexes. To gain more useful information about the relative binding strengths of the different ligands present in the ditopic ligands (**L1** and **L2**), a series of competition experiments were performed using the analogous model ligands and complexes (Supporting Information, Figures S59−S75).

Given the κ^2-tripy coordination mode in the diCu(I) complexes of the ditopic ligands, we attempted the synthesis of the model [Cu(κ^2-tripy)(diMesbpy)](PF$_6$). Under an inert atmosphere, [Cu(MeCN)$_4$](PF$_6$) and diMesbpy were stirred in acetone followed by addition of the tripy ligand; addition of diethyl ether gave the complex as an orange powder. HRESI-MS data displayed a peak at m/z = 848.3265 that was consistent with the presence of the cationic species [Cu(κ^2-tripy)(diMesbpy)]$^+$. ^{1}H NMR spectroscopy provided evidence for the formation of the desired [Cu(κ^2-tripy)(diMesbpy)]-(PF$_6$) complex (Figure 10), with the spectrum showing one set

https://doi.org/10.1021/acsomega.1c04977
ACS Omega 2021, 6, 30115−30129

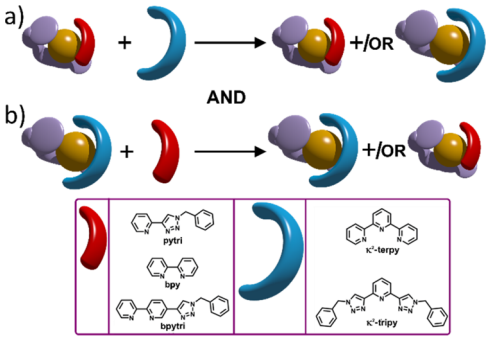

Figure 11. (a, b) Cartoon representation of the competition study along with the ligands used.

of well-defined resonances that are not paramagnetically shifted characteristic of a Cu(I) species. The spectrum was symmetrical (only one set of resonances is observed for the 1,2,3-triazole units), suggesting that the complex is fluxional at room temperature with the $[Cu(diMesbpy)]^+$ unit "flipping" between the two bidentate pytri binding sites (Figure 10). Variable temperature (VT) ^{1}H NMR experiments were carried out in an effort to slow the exchange process. However, the ^{1}H NMR spectra of the complex remain symmetric down to −40 °C, suggesting that the barrier to the exchange process is small (Supporting Information, Figure S49). The hypodentate κ^2-coordination mode of the tripy ligand was ultimately confirmed by X-ray crystallography (Figure 10 and the Supporting Information, Figure S57). The molecular structure of the complex was solved in the monoclinic $P2_1/n$ space group and exhibited the expected four-coordinate arrangement about the Cu(I) ion (Figure 10). Akin to the $[Cu_2(\mathbf{L2})(diMesbpy)_2](PF_6)_2$ complex, one of the triazole arms of the tripy ligand is rotated ∼180° such that the triazole proton is pointed toward the Cu(I) ion. Similar to the other pytri and κ^2-tripy copper(I) complexes, the structure displays a distorted tetrahedral geometry (τ_4 = 0.74) about the copper(I) ion (Figure 10).

With all the required model complexes in hand, we carried out a series of competition experiments to further examine the relative ligand binding strengths. Two different approaches were undertaken: either a preformed $[(diMesbpy)copper(I)(N{-}N)]^+$ complex (where N−N = pytri, bpytri or bpy) was treated with a nominally tridentate ligand (tripy or terpy), or a preformed $[(diMesbpy)copper(I)(\kappa^2\text{-}N{-}N{-}N)]^+$ complex (where N−N−N = tripy or terpy) was treated with a bidentate ligand (pytri, bpytri or bpy) (Figure 11). The competition experiments were carried out (in triplicate) in d_6-acetone at 298 K in the presence of a tetrakis(trimethylsilyl)silane internal standard. After thorough mixing, the solutions were analyzed by ^{1}H NMR spectroscopy and HRESI-MS under pseudo cryospray conditions (−10 °C) (Figure 12 and the Supporting Information, Figures S59−S75).

HRESI-MS data from all the competition mixtures showed the presence of the two partner copper(I) complexes (Supporting Information and Figure 12 and Table 1), indicating that, in each case, some ligand exchange is occurring. For example, the mixture of $[Cu(pytri)(diMesbpy)](PF_6)$ and tripy displayed two major peaks at m/z = 691.2796 and 848.3384, consistent with the presence of $[Cu(pytri)(diMesbpy)]^+$ and $[Cu(\kappa^2\text{-tripy})(diMesbpy)]^+$, respectively. Smaller peaks due to free tripy and pytri were also detected. The amount of ligand exchange was quantified using the ^{1}H NMR spectra of the mixtures (Supporting Information and Figure 12 and Table 1). The spectra of the model systems were considerably less complex than those of the ditopic ligands (**L1** and **L2**) and were typically a superimposition of the reactants and any exchange complex. Thus, a simple analysis of the complex integrals enabled the ratio of the copper(I) complexes to be determined (Supporting Information and Table 1). For example, analysis of the $[Cu(pytri)(diMesbpy)](PF_6)$ and tripy competition experiment indicated that a 74:26 mixture of $[Cu(pytri)(diMesbpy)](PF_6)$:$[Cu(\kappa^2\text{-tripy})(diMesbpy)](PF_6)$ was obtained (Supporting Information and Figure 12 and Table 1). Consistently, a 76:24 ratio was obtained from the mixture of $[Cu(\kappa^2\text{-tripy})(diMesbpy)](PF_6)$ and pytri (Supporting Information, Figure S59 and Table 1). We note that the observed (essentially) 3:1 ratio of the two copper(I) complexes is very similar to the 2:1 mixtures of co-conformational isomers observed by Goldup and co-workers in their [2]rotaxane (Figure 2).[69] Similar competition experiments with the bpytri or bpy ligands (Table 1) showed that increasing the donor strength of the bidentate ligand led to better selectivity for the formation of the $[(diMesbpy)copper(I)(N{-}N)]^+$ over the $[(diMesbpy)copper(I)(\kappa^2\text{-}N{-}N{-}N)]^+$ complex, but with those ligand combinations, a 9:1 mixture was obtained (Table 1). The $[Cu(pytri)(diMesbpy)](PF_6)$, $[Cu(bpytri)(diMesbpy)](PF_6)$, and $[Cu(bpy)(diMesbpy)](PF_6)$ were also treated with terpy as terpy is also known to be able to adopt the κ^2-bidentate coordination mode.[71,80] Interestingly, the $[(diMesbpy)copper(I)(N{-}N)]^+$:$[(diMesbpy)copper(I)(\kappa^2\text{-}N{-}N{-}N)]^+$ ratios observed were very similar to those obtained with tripy, suggesting that it is the weaker binding strength of the pytri unit that is the major contributor to the lack of selectivity observed in these systems.

CONCLUSIONS

Herein, we have examined if the more readily synthesized bidentate Rpytri and tridentate Rtripy click ligands can be used to develop a selective Cu(I/II) switching mechanism enabling them to replace more common polypyridine bpy/phen and terpy ligand partners. We generated two new ditopic ligands that feature bidentate (pytri, **L1** or bpytri, **L2**) and tridentate tripy metal binding pockets. We examined the coordination chemistry of those ligands with copper(I) and copper(II) diMesbpy units. Additionally, we synthesized a family of model complexes and used an array of techniques, NMR and UV−vis spectroscopies, HRESI-MS, and X-ray crystallography, to examine the behavior of the compounds. We showed that **L1** and **L2** formed $[(diMesbpy)Cu(\mathbf{L1}\text{ or }\mathbf{L2})]^{2+}$ complexes where the copper(II) diMesbpy unit was coordinated exclusively in the tridentate tripy binding site. However, with copper(I) diMesbpy units, a mixture of complexes was obtained. NMR and MS data indicated that a 1:1 mixture of $[Cu(diMesbpy)]^+$ and either **L1** or **L2** generates three complexes in solution, the dimetallic $[(diMesbpy)_2Cu_2(\mathbf{L1}\text{ or }\mathbf{L2})]^{2+}$ and the monometallic isomers of $[(diMesbpy)Cu(\mathbf{L1}\text{ or }\mathbf{L2})]^+$ where the $[Cu(diMesbpy)]^+$ unit is coordinated to either the bidentate or tridentate binding sites of the ditopic ligands. The dimetallic $[(diMesbpy)_2Cu_2(\mathbf{L1}\text{ or }\mathbf{L2})](PF_6)_2$ complexes were synthesized independently, and the molecular structures were obtained using X-ray crystallography. Both complexes feature a $[Cu(diMesbpy)]^+$ coordinated to the bidentate (pytri or bpytri) pocket of the ditopic ligands (**L1** or **L2**), as expected. They also feature a second $[Cu(diMesbpy)]^+$ coordinated to the nominally tridentate tripy binding site in a

https://doi.org/10.1021/acsomega.1c04977
ACS Omega 2021, 6, 30115−30129

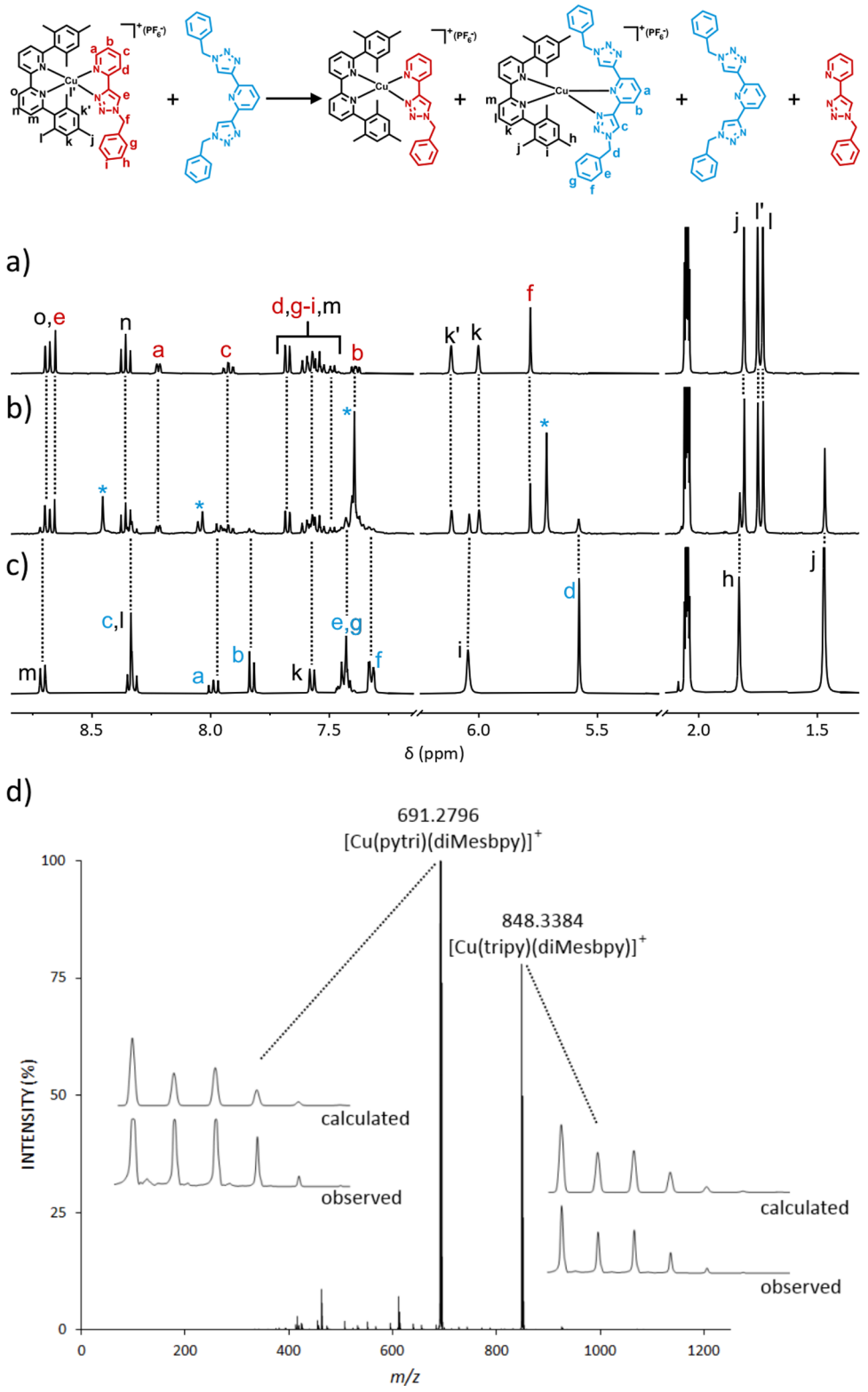

Figure 12. Scheme for the competition study carried out using [Cu(pytri)(diMesbpy)](PF$_6$) and tripy. Also shown are the stacked partial ^{1}H NMR (400 MHz, d_6-acetone, 298 K) spectra: (a) [Cu(pytri)(diMesbpy)](PF$_6$), (b) the mixture of [Cu(pytri)(diMesbpy)](PF$_6$) and the tripy ligand, and (c) [Cu(κ^2-tripy)(diMesbpy)](PF$_6$). Dotted lines show that the species in the top and bottom spectra are present in the middle spectrum. Resonances for noncomplexed tripy marked with asterisks (*). (d) Pseudo cryospray HRESI-MS (acetone/MeOH) of the Cu(I) competition mixture ([Cu(pytri)(diMesbpy)](PF$_6$) and tripy).

four-coordinate hypodenate κ^2-fashion. This behavior was examined further using competition experiments, which showed that a 3:1 mixture of $[Cu(pytri)(diMesbpy)]^+$ and $[Cu(\kappa^2\text{-tripy})(diMesbpy)]^+$ was generated, confirming that the κ^2-tripy bidentate coordination mode displays a similar binding strength to the related pytri ligand. Changing the bidentate

https://doi.org/10.1021/acsomega.1c04977
ACS Omega 2021, 6, 30115−30129

Table 1. Mixtures of Complexes and Competing Ligands Used in the Cu(I) Competition Studies as well as the Results from ^{1}H NMR Spectroscopy and Pseudo Cryospray HRESI-MS

initial complex	competing ligand	ratio from ^{1}H NMR spectroscopy[a]	species detected using HRESI-MS
[Cu(pytri)(diMesbpy)](PF$_6$)	tripy	74:26	[Cu(pytri)(diMesbpy)]$^+$
			[Cu(κ^2-tripy)(diMesbpy)]$^+$
[Cu(κ^2-tripy)(diMesbpy)](PF$_6$)	pytri	24:76	[Cu(κ^2-tripy)(diMesbpy)]$^+$
			[Cu(pytri)(diMesbpy)]$^+$
[Cu(bpytri)(diMesbpy)](PF$_6$)	tripy	90:10	[Cu(bpytri)(diMesbpy)]$^+$
			[Cu(κ^2-tripy)(diMesbpy)]$^+$
[Cu(κ^2-tripy)(diMesbpy)](PF$_6$)	bpytri	8:92	[Cu(κ^2-tripy)(diMesbpy)]$^+$
			[Cu(bpytri)(diMesbpy)]$^+$
[Cu(bpy)(diMesbpy)](PF$_6$)	tripy	91:9	[Cu(bpy)(diMesbpy)]$^+$
			[Cu(κ^2-tripy)(diMesbpy)]$^+$
[Cu(κ^2-tripy)(diMesbpy)](PF$_6$)	bpy	7:93	[Cu(κ^2-tripy)(diMesbpy)]$^+$
			[Cu(bpy)(diMesbpy)]$^+$
[Cu(pytri)(diMesbpy)](PF$_6$)	terpy	75:25	[Cu(pytri)(diMesbpy)]$^+$
			[Cu(κ^2-terpy)(diMesbpy)]$^+$
[Cu(bpytri)(diMesbpy)](PF$_6$)	terpy	93:7	[Cu(bpytri)(diMesbpy)]$^+$
			[Cu(κ^2-terpy)(diMesbpy)]$^+$
[Cu(bpy)(diMesbpy)](PF$_6$)	terpy	95:5	[Cu(bpy)(diMesbpy)]$^+$
			[Cu(κ^2-terpy)(diMesbpy)]$^+$

[a]Ratio of the initial complex:exchange complex.

binding site to a stronger donor ligand leads to better selectivity in solution with a 9:1 mixture of the [Cu(N−N)(diMesbpy)]$^+$ and [Cu(κ^2-N−N−N)(diMesbpy)]$^+$ complexes obtained. Overall, the results suggest that the pytri/tripy and bpytri/tripy ligand pairs cannot be used as replacements for the more common bpy/phen-terpy partners due to the lack of selectivity in the copper(I) state. However, the results obtained do suggest that the tridentate tripy unit could be incorporated in a selective Cu(I)/Cu(II) switch if partnered with a suitably stronger bidentate ligand. Additionally, we have shown that tripy ligands can readily adopt a κ^2-bidentate coordination mode, while similar behavior has been known for terpy systems for some time;[71] this potentially opens up new avenues for tripy coordination chemistry.[63]

■ ASSOCIATED CONTENT

Supporting Information

The Supporting Information is available free of charge at https://pubs.acs.org/doi/10.1021/acsomega.1c04977.

Experimental section, ^{1}H, ^{13}C, and 2D NMR spectral data, HRESI-MS, UV−vis, and X-ray data (PDF)

Crystallographic information (including CIF files, CCDC numbers 2065119, 2065122, 2065120, 2065123, 2094328, and 2094327) (CIF)

■ AUTHOR INFORMATION

Corresponding Author

James D. Crowley − *Department of Chemistry, University of Otago, Dunedin 9054, New Zealand; MacDiarmid Institute for Advanced Materials and Nanotechnology, Wellington 6140, New Zealand;* orcid.org/0000-0002-3364-2267; Email: jcrowley@chemistry.otago.ac.nz

Authors

Daniel A. W. Ross − *Department of Chemistry, University of Otago, Dunedin 9054, New Zealand; MacDiarmid Institute for Advanced Materials and Nanotechnology, Wellington 6140, New Zealand*

James A. Findlay − *Department of Chemistry, University of Otago, Dunedin 9054, New Zealand; MacDiarmid Institute for Advanced Materials and Nanotechnology, Wellington 6140, New Zealand*

Roan A. S. Vasdev − *Department of Chemistry, University of Otago, Dunedin 9054, New Zealand; MacDiarmid Institute for Advanced Materials and Nanotechnology, Wellington 6140, New Zealand*

Complete contact information is available at: https://pubs.acs.org/10.1021/acsomega.1c04977

Notes

The authors declare no competing financial interest.

The manuscript was written through contributions of all authors. All authors have given approval to the final version of the manuscript.

■ ACKNOWLEDGMENTS

This work was supported by the Department of Chemistry, University of Otago and MacDiarmid Institute. D.A.W.R., J.A.F., and R.A.S.V. thank the University of Otago for doctoral scholarships. D.A.W.R. and R.A.S.V. thank the MacDiarmid Institute for COVID19 doctoral scholarship extensions. J.A.F. thanks the MacDiarmid Institute for funding a research assistant position. D.A.W.R. also thanks the University of Otago for a publishing bursary.

■ ABBREVIATIONS

bpy, 2,2′-bipyridine; bpytri, 5-(1-benzyl-1*H*-1,2,3-triazol-4-yl)-2,2′-bipyridine; CuAAC, copper(I)-catalyzed azide-alkyne cycloaddition; DCM, dichloromethane; diMesbpy, 6,6′-dimesityl-2,2′-bipyridine; DMF, *N*,*N*′-dimethylformamide; DMSO, dimethylsulfoxide; equiv, equivalent(s); HETPHEN, heteroleptic bisphenanthroline complexation; HRESI-MS, high-resolution electrospray ionization mass spectrometry; MeCN, acetonitrile; MeOH, methanol; NMR, nuclear magnetic resonance; OTs, tosylate; phen, 1,10-phenanthroline; pytri, 2-(1-benzyl-1*H*-1,2,3-triazol-4-yl)pyridine; RT, room temperature; terpy, 2,2′:6′2″-terpyridine; TMS, trimethylsilane; tripy, 2,6-bis(1-benzyl-1*H*-1,2,3-triazol-4-yl)pyridine; UV−vis, ultraviolet−visible

■ REFERENCES

(1) Ayme, J.-F.; Beves, J. E.; Campbell, C. J.; Leigh, D. A. Template synthesis of molecular knots. *Chem. Soc. Rev.* **2013**, *42*, 1700−1712.

(2) Beves, J. E.; Blight, B. A.; Campbell, C. J.; Leigh, D. A.; McBurney, R. T. Strategies and Tactics for the Metal-Directed Synthesis of Rotaxanes, Knots, Catenanes, and Higher Order Links. *Angew. Chem., Int. Ed.* **2011**, *50*, 9260−9327.
(3) Crowley, J. D.; Goldup, S. M.; Lee, A.-L.; Leigh, D. A.; McBurney, R. T. Active metal template synthesis of rotaxanes, catenanes and molecular shuttles. *Chem. Soc. Rev.* **2009**, *38*, 1530−1541.
(4) Bruns, C. J.; Stoddart, J. F., *Nature of the Mechanical Bond: From Molecules to Machines*; John Wiley & Sons, Inc.: 2016; p 786 pp.
(5) Lewis, J. E. M.; Galli, M.; Goldup, S. M. Properties and emerging applications of mechanically interlocked ligands. *Chem. Commun.* **2017**, *53*, 298−312.
(6) Bruns, C. J.; Stoddart, J. F. The mechanical bond: a work of art. *Top. Curr. Chem.* **2011**, *323*, 19−27. (Beauty in Chemistry: Artistry in the Creation of New Molecules),
(7) Barin, G.; Forgan, R. S.; Stoddart, J. F. Mechanostereochemistry and the mechanical bond. *Proc. R. Soc. A* **2012**, *468*, 2849−2880.
(8) Stoddart, J. F. The chemistry of the mechanical bond. *Chem. Soc. Rev.* **2009**, *38*, 1802−1820.
(9) Griffiths, K. E.; Stoddart, J. F. Template-directed synthesis of donor/acceptor [2]catenanes and [2]rotaxanes. *Pure Appl. Chem.* **2008**, *80*, 485−506.
(10) Dichtel, W. R.; Miljanić, O. Š.; Zhang, W.; Spruell, J. M.; Patel, K.; Aprahamian, I.; Heath, J. R.; Stoddart, J. F. Kinetic and Thermodynamic Approaches for the Efficient Formation of Mechanical Bonds. *Acc. Chem. Res.* **2008**, *41*, 1750−1761.
(11) Chambron, J.-C.; Sauvage, J.-P. Topologically complex molecules obtained by transition metal templation: it is the presentation that determines the synthesis strategy. *New J. Chem.* **2013**, *37*, 49−57.
(12) Forgan, R. S.; Sauvage, J.-P.; Stoddart, J. F. Chemical Topology: Complex Molecular Knots, Links, and Entanglements. *Chem. Rev.* **2011**, *111*, 5434−5464.
(13) Dattler, D.; Fuks, G.; Heiser, J.; Moulin, E.; Perrot, A.; Yao, X.; Giuseppone, N. Design of Collective Motions from Synthetic Molecular Switches, Rotors, and Motors. *Chem. Rev.* **2020**, *120*, 310−433.
(14) Lancia, F.; Ryabchun, A.; Katsonis, N. Life-like motion driven by artificial molecular machines. *Nat. Rev. Chem.* **2019**, *3*, 536−551.
(15) Zhang, L.; Marcos, V.; Leigh, D. A. Molecular machines with bio-inspired mechanisms. *Proc. Natl. Acad. Sci. U. S. A.* **2018**, *115*, 9397−9404.
(16) Kassem, S.; van Leeuwen, T.; Lubbe, A. S.; Wilson, M. R.; Feringa, B. L.; Leigh, D. A. Artificial molecular motors. *Chem. Soc. Rev.* **2017**, *46*, 2592−2621.
(17) Leigh, D. A. Genesis of the Nanomachines: The 2016 Nobel Prize in Chemistry. *Angew. Chem., Int. Ed.* **2016**, *55*, 14506−14508.
(18) Kay, E. R.; Leigh, D. A. Rise of the Molecular Machines. *Angew. Chem., Int. Ed.* **2015**, *54*, 10080−10088.
(19) Erbas-Cakmak, S.; Leigh, D. A.; McTernan, C. T.; Nussbaumer, A. L. Artificial Molecular Machines. *Chem. Rev.* **2015**, *115*, 10081−10206.
(20) Kay, E. R.; Leigh, D. A.; Zerbetto, F. Synthetic Molecular Motors and Mechanical Machines. *Angew. Chem., Int. Ed.* **2007**, *46*, 72−191.
(21) Pezzato, C.; Cheng, C.; Stoddart, J. F.; Astumian, R. D. Mastering the non-equilibrium assembly and operation of molecular machines. *Chem. Soc. Rev.* **2017**, *46*, 5491−5507.
(22) Cheng, C.; Stoddart, J. F. Wholly Synthetic Molecular Machines. *ChemPhysChem* **2016**, *17*, 1780−1793.
(23) Bruns, C. J.; Stoddart, J. F. Rotaxane-Based Molecular Muscles. *Acc. Chem. Res.* **2014**, *47*, 2186−2199.
(24) Browne, W. R.; Feringa, B. L. Making molecular machines work. *Nat. Nanotechnol.* **2006**, *1*, 25−35.
(25) Jeong, M.; Park, J.; Kwon, S. Molecular Switches and Motors Powered by Orthogonal Stimuli. *Eur. J. Org. Chem.* **2020**, *2020*, 7254−7283.
(26) Stoddart, J. F. Mechanically Interlocked Molecules (MIMs)-Molecular Shuttles, Switches, and Machines (Nobel Lecture). *Angew. Chem., Int. Ed.* **2017**, *56*, 11094−11125.
(27) Feringa, B. L. The Art of Building Small: From Molecular Switches to Motors (Nobel Lecture). *Angew. Chem., Int. Ed.* **2017**, *56*, 11060−11078.
(28) Sauvage, J. P. From Chemical Topology to Molecular Machines (Nobel Lecture). *Angew. Chem., Int. Ed.* **2017**, *56*, 11080−11093.
(29) McConnell, A. J.; Wood, C. S.; Neelakandan, P. P.; Nitschke, J. R. Stimuli-Responsive Metal-Ligand Assemblies. *Chem. Rev.* **2015**, *115*, 7729−7793.
(30) Goswami, A.; Saha, S.; Biswas, P. K.; Schmittel, M. (Nano)mechanical Motion Triggered by Metal Coordination: from Functional Devices to Networked Multicomponent Catalytic Machinery. *Chem. Rev.* **2020**, *120*, 125−199.
(31) Zanetti-Polzi, L.; Djemili, R.; Durot, S.; Heitz, V.; Daidone, I.; Ventura, B. Allosteric Control of Naphthalene Diimide Encapsulation and Electron Transfer in Porphyrin Containers: Photophysical Studies and Molecular Dynamics Simulation. *Chem. − Eur. J.* **2020**, *26*, 17514−17524.
(32) Djemili, R.; Kocher, L.; Durot, S.; Peuronen, A.; Rissanen, K.; Heitz, V. Positive Allosteric Control of Guests Encapsulation by Metal Binding to Covalent Porphyrin Cages. *Chem. − Eur. J.* **2018**, *25*, 1481−1487.
(33) Schoepff, L.; Kocher, L.; Durot, S.; Heitz, V. Chemically Induced Breathing of Flexible Porphyrinic Covalent Cages. *J. Org. Chem.* **2017**, *82*, 5845−5851.
(34) Noor, A.; Maloney, D. L.; Lewis, J. E. M.; Lo, W. K. C.; Crowley, J. D. Acid-Base Driven Ligand Exchange with Palladium(II) ″Click″ Complexes. *Asian J. Org. Chem.* **2015**, *4*, 208−211.
(35) Crowley, J. D.; Leigh, D. A.; Lusby, P. J.; McBurney, R. T.; Perret-Aebi, L.-E.; Petzold, C.; Slawin, A. M. Z.; Symes, M. D. A Switchable Palladium-Complexed Molecular Shuttle and Its Metastable Positional Isomers. *J. Am. Chem. Soc.* **2007**, *129*, 15085−15090.
(36) Beves, J. E.; Blanco, V.; Blight, B. A.; Carrillo, R.; D'Souza, D. M.; Howgego, D.; Leigh, D. A.; Slawin, A. M. Z.; Symes, M. D. Toward Metal Complexes That Can Directionally Walk Along Tracks: Controlled Stepping of a Molecular Biped with a Palladium-(II) Foot. *J. Am. Chem. Soc.* **2014**, *136*, 2094−2100.
(37) Sooksawat, D.; Pike, S. J.; Slawin, A. M. Z.; Lusby, P. J. Acid-base responsive switching between ″3+1″ and ″2+2″ platinum complexes. *Chem. Commun.* **2013**, *49*, 11077−11079.
(38) Pike, S. J.; Lusby, P. J. Dual stimuli-responsive interconvertible heteroleptic platinum coordination modes. *Chem. Commun.* **2010**, *46*, 8338−8340.
(39) Lusby, P. J.; Muller, P.; Pike, S. J.; Slawin, A. M. Z. Stimuli-Responsive Reversible Assembly of 2D and 3D Metallosupramolecular Architectures. *J. Am. Chem. Soc.* **2009**, *131*, 16398−16400.
(40) Livoreil, A.; Dietrich-Buchecker, C. O.; Sauvage, J.-P. Electrochemically Triggered Swinging of a [2]-Catenate. *J. Am. Chem. Soc.* **1994**, *116*, 9399−9400.
(41) Livoreil, A.; Sauvage, J.-P.; Armaroli, N.; Balzani, V.; Flamigni, L.; Ventura, B. Electrochemically and Photochemically Driven Ring Motions in a Disymmetrical Copper [2]-Catenate. *J. Am. Chem. Soc.* **1997**, *119*, 12114−12124.
(42) Armaroli, N.; Balzani, V.; Collin, J.-P.; Gaviña, P.; Sauvage, J.-P.; Ventura, B. Rotaxanes Incorporating Two Different Coordinating Units in Their Thread: Synthesis and Electrochemically and Photochemically Induced Molecular Motions. *J. Am. Chem. Soc.* **1999**, *121*, 4397−4408.
(43) Durola, F.; Sauvage, J.-P. Fast Electrochemically Induced Translation of the Ring in a Copper-Complexed [2]Rotaxane: The Biisoquinoline Effect. *Angew. Chem., Int. Ed.* **2007**, *46*, 3537−3540.
(44) Raehm, L.; Kern, J.-M.; Sauvage, J.-P. A Transition Metal Containing Rotaxane in Motion: Electrochemically Induced Pirouetting of the Ring on the Threaded Dumbbell. *Chem. − Eur. J.* **1999**, *5*, 3310−3317.

https://doi.org/10.1021/acsomega.1c04977
ACS Omega 2021, 6, 30115−30129

(45) Poleschak, I.; Kern, J.-M.; Sauvage, J.-P. A copper-complexed rotaxane in motion: pirouetting of the ring on the millisecond timescale. *Chem. Commun.* **2004**, *4*, 474−476.
(46) Létinois-Halbes, U.; Hanss, D.; Beierle, J. M.; Collin, J.-P.; Sauvage, J.-P. A Fast-Moving [2]Rotaxane Whose Stoppers Are Remote from the Copper Complex Core. *Org. Lett.* **2005**, *7*, 5753−5756.
(47) Joosten, A.; Trolez, Y.; Collin, J.-P.; Heitz, V.; Sauvage, J.-P. Copper(I)-Assembled [3]Rotaxane Whose Two Rings Act as Flapping Wings. *J. Am. Chem. Soc.* **2012**, *134*, 1802−1809.
(48) Samanta, S. K.; Rana, A.; Schmittel, M. Reversible cargo shipping between orthogonal stations of a nanoscaffold upon redox input. *Dalton Trans.* **2014**, *43*, 9438−9447.
(49) Scottwell, S. Ø.; Barnsley, J. E.; McAdam, C. J.; Gordon, K. C.; Crowley, J. D. A ferrocene based switchable molecular folding ruler. *Chem. Commun.* **2017**, *53*, 7628−7631.
(50) Scottwell, S. Ø.; Elliott, A. B. S.; Shaffer, K. J.; Nafady, A.; McAdam, C. J.; Gordon, K. C.; Crowley, J. D. Chemically and electrochemically induced expansion and contraction of a ferrocene rotor. *Chem. Commun.* **2015**, *51*, 8161−8164.
(51) Benson, C. R.; Share, A. I.; Marzo, M. G.; Flood, A. H. Double Switching of Two Rings in Palindromic [3]Pseudorotaxanes: Cooperativity and Mechanism of Motion. *Inorg. Chem.* **2016**, *55*, 3767−3776.
(52) Share, A. I.; Parimal, K.; Flood, A. H. Bilability is Defined when One Electron is Used to Switch between Concerted and Stepwise Pathways in Cu(I)-Based Bistable [2/3]Pseudorotaxanes. *J. Am. Chem. Soc.* **2010**, *132*, 1665−1675.
(53) Parimal, K.; Witlicki, E. H.; Flood, A. H. Interconverting Two Classes of Architectures by Reduction of a Self-Sorting Mixture. *Angew. Chem., Int. Ed.* **2010**, *49*, 4628−4632.
(54) Schmittel, M.; De, S.; Pramanik, S. Reversible ON/OFF Nanoswitch for Organocatalysis: Mimicking the Locking and Unlocking Operation of CaMKII. *Angew. Chem., Int. Ed.* **2012**, *51*, 3832−3836.
(55) De, S.; Pramanik, S.; Schmittel, M. A monomer−dimer nanoswitch that mimics the working principle of the SARS-CoV 3CLpro enzyme controls copper-catalysed cyclopropanation. *Dalton Trans.* **2014**, *43*, 10977−10982.
(56) Haberhauer, G. A Metal-Ion-Driven Supramolecular Chirality Pendulum. *Angew. Chem., Int. Ed.* **2010**, *49*, 9286−9289.
(57) Haberhauer, G. Control of Planar Chirality: The Construction of a Copper-Ion-Controlled Chiral Molecular Hinge. *Angew. Chem., Int. Ed.* **2008**, *47*, 3635−3638.
(58) van Hilst, Q. V. C.; Lagesse, N. R.; Preston, D.; Crowley, J. D. Functional metal complexes from CuAAC ″click″ bidentate and tridentate pyridyl-1,2,3-triazole ligands. *Dalton Trans.* **2018**, 997.
(59) Crowley, J. D.; McMorran, D. A. ″Click-triazole″ coordination chemistry: exploiting 1,4-disubstituted-1,2,3-triazoles as ligands. *Top. Heterocycl. Chem.* **2012**, *28*, 31−83.
(60) Struthers, H.; Mindt, T. L.; Schibli, R. Metal chelating systems synthesized using the copper(I) catalyzed azide-alkyne cycloaddition. *Dalton Trans.* **2010**, *39*, 675−696.
(61) Vasdev, R. A. S.; Preston, D.; Crowley, J. D. Functional metallosupramolecular architectures using 1,2,3-triazole ligands: it's as easy as 1,2,3 ″click″. *Dalton Trans.* **2017**, *46*, 2402−2414.
(62) Scattergood, P. A.; Sinopoli, A.; Elliott, P. I. P. Photophysics and photochemistry of 1,2,3-triazole-based complexes. *Coord. Chem. Rev.* **2017**, *350*, 136−154.
(63) Byrne, J. P.; Kitchen, J. A.; Gunnlaugsson, T. The btp [2,6-bis(1,2,3-triazol-4-yl)pyridine] binding motif: a new versatile terdentate ligand for supramolecular and coordination chemistry. *Chem. Soc. Rev.* **2014**, *43*, 5302−5325.
(64) Li, Y.; Huffman, J. C.; Flood, A. H. Can terdentate 2,6-bis(1,2,3-triazol-4-yl)pyridines form stable coordination compounds? *Chem. Commun.* **2007**, *26*, 2692−2694.
(65) Meldal, M.; Tornoe, C. W. Cu-Catalyzed Azide-Alkyne Cycloaddition. *Chem. Rev.* **2008**, *108*, 2952−3015.
(66) Cirulli, M.; Kaur, A.; Lewis, J. E. M.; Zhang, Z.; Kitchen, J. A.; Goldup, S. M.; Roessler, M. M. Rotaxane-Based Transition Metal Complexes: Effect of the Mechanical Bond on Structure and Electronic Properties. *J. Am. Chem. Soc.* **2019**, *141*, 879−889.
(67) Byrne, J. P.; Blasco, S.; Aletti, A. B.; Hessman, G.; Gunnlaugsson, T. Formation of Self-Templated 2,6-Bis(1,2,3-triazol-4-yl)pyridine [2]Catenanes by Triazolyl Hydrogen Bonding: Selective Anion Hosts for Phosphate. *Angew. Chem., Int. Ed.* **2016**, *55*, 8938−8943.
(68) Lewis, J. E. M.; Modicom, F.; Goldup, S. M. Efficient Multicomponent Active Template Synthesis of Catenanes. *J. Am. Chem. Soc.* **2018**, *140*, 4787−4791.
(69) Lewis, J. E. M.; Bordoli, R. J.; Denis, M.; Fletcher, C. J.; Galli, M.; Neal, E. A.; Rochette, E. M.; Goldup, S. M. High yielding synthesis of 2,2′-bipyridine macrocycles, versatile intermediates in the synthesis of rotaxanes. *Chem. Sci.* **2016**, *7*, 3154−3161.
(70) Blackman, A. G. Overcoming the chelate effect: hypodentate coordination of common multidentate amine ligands. *C. R. Chim.* **2005**, *8*, 107−119.
(71) Constable, E. C.; Housecroft, C. E. More hydra than Janus − Non-classical coordination modes in complexes of oligopyridine ligands. *Coord. Chem. Rev.* **2017**, *350*, 84−104.
(72) Schmittel, M.; Ganz, A.; Schenk, W. A.; Hagel, M. Synthesis and coordination properties of 6,6′-dimesityl-2,2′-bipyridine. *Z. Naturforsch., B: Chem. Sci.* **1999**, *54*, 559−564.
(73) Mapley, J. I.; Ross, D. A. W.; McAdam, C. J.; Gordon, K. C.; Crowley, J. D. Triphenylamine-substituted 2-pyridyl-1,2,3-triazole copper(I) complexes: an experimental and computational investigation. *J. Coord. Chem.* **2019**, *72*, 1378−1394.
(74) Crowley, J. D.; Bandeen, P. H.; Hanton, L. R. A one pot multicomponent CuAAC ″click″ approach to bidentate and tridentate pyridyl-1,2,3-triazole ligands: synthesis, x-ray structures and copper(II) and silver(I) complexes. *Polyhedron* **2010**, *29*, 70−83.
(75) Cote, C.; Kirss, R. U. Rhenium tricarbonyl complexes of 1-benzyl-4-(5-bipyridyl)-1H-1,2,3-triazoles. *Inorg. Chim. Acta* **2010**, *363*, 2520−2525.
(76) Yang, L.; Powell, D. R.; Houser, R. P. Structural variation in copper(I) complexes with pyridylmethylamide ligands: structural analysis with a new four-coordinate geometry index, τ_4. *Dalton Trans.* **2007**, *9*, 955−964.
(77) Addison, A. W.; Rao, T. N.; Reedijk, J.; van Rijn, J.; Verschoor, G. C. Synthesis, structure, and spectroscopic properties of copper(II) compounds containing nitrogen-sulphur donor ligands; the crystal and molecular structure of aqua[1,7-bis(N-methylbenzimidazol-2′-yl)-2,6-dithiaheptane]copper(II) perchlorate. *J. Chem. Soc., Dalton Trans.* **1984**, 1349−1356.
(78) Lewis, J. E. M.; Elliott, A. B. S.; McAdam, C. J.; Gordon, K. C.; Crowley, J. D. 'Click' to functionalise: synthesis, characterisation and enhancement of the physical properties of a series of exo- and endo-functionalised Pd_2L_4 nanocages. *Chem. Sci.* **2014**, *5*, 1833−1843.
(79) Lo, W. K. C.; Huff, G. S.; Cubanski, J. R.; Kennedy, A. D. W.; McAdam, C. J.; McMorran, D. A.; Gordon, K. C.; Crowley, J. D. Comparison of Inverse and Regular 2-Pyridyl-1,2,3-triazole "Click" Complexes: Structures, Stability, Electrochemical, and Photophysical Properties. *Inorg. Chem.* **2015**, *54*, 1572−1587.
(80) Goswami, A.; Schmittel, M. Double Rotors with Fluxional Axles: Domino Rotation and Azide-Alkyne Huisgen Cycloaddition Catalysis. *Angew. Chem., Int. Ed.* **2020**, *59*, 12362−12366.

https://doi.org/10.1021/acsomega.1c04977
ACS Omega 2021, 6, 30115−30129